UNIVERSITY OF CALIFORNIA
Santa Barbara

TEMPORAL CALIBRATION SENSITIVITY OF THE SLEUTH URBAN GROWTH MODEL

A thesis submitted in partial fulfillment of the requirements for the degree of Master of Arts

in Geography

by

Jeannette Therese Candau

Committee in charge:

Professor Keith C. Clarke

Professor Helen Couclelis

Steen Rassmussen Ph.D.

June 2002

This thesis of Jeannette Therese Candau is approved.

_____

_____

_____

Committee Chairperson

Abstract

Temporal Calibration Sensitivity of the SLEUTH Urban Growth Model

by

Jeannette Therese Candau

SLEUTH is a coupled cellular automata model of urban and other land cover change. This research focuses only on the urban component of the model. SLEUTH was calibrated using historical urban and land cover data that aid in obtaining an ideal set of parameters for forecasting land cover change. The oldest data sets were used to initialize the model and subsequent, or "control," data were used for goodness-of-fit measurements over time. Due to the considerable computation required for calibration, previous research has implemented a "brute force" calibration methodology that steps through parameter ranges and spatial resolution at different scales in three phases, from rough to fine-grain. The area in and around the city of Santa Barbara, California, was used to examine the sensitivity of this calibration process to scaling. Urban areas were defined by identifying and digitizing built structures from aerial photography for the years 1929, 1943, 1956, 1967, 1976, 1986, and 1998 in a geographic information system. These digitized layers were then converted to raster format at a spatial resolution of 30 m. Multiple calibrations of the model were executed by varying the temporal and spatial resolution of the input data set. First, it was found that SLEUTH calibration is not scalable across image resolutions. Secondly, for Santa Barbara, decadal data from the last forty years proved more effective for calibration than including the entire historical profile. These findings point to more effective and efficient calibration methods of SLEUTH as well as other cellular automata based land cover models.

TABLE OF CONTENTS

LIST OF FIGURES

ACKNOWLEDGMENTS

My sojourn to completion of my Masters has taken much time and involved contact with many individuals whom I would like to acknowledge.

The U. S. Geological Survey has always provided excellent financial and research support for which I am extremely grateful. The now Geographic Analysis and Monitoring Program (previously Urban Dynamics) has brought me into contact with research collaborators who provided much assistance, support and humor: William Acevedo, Lora Richards, Len Gaydos, Dave Hester, Mark Feller and the ever lovin' Bun Boy. Special thanks to Tommy Cathey, without whom I'd doubtlessly still be wallowing in C code.

Thanks to Keith Clarke for all of his creativity, encouragement, patience, and challenge. My other committee members Steen Rassmussen and Helen Couclelis have provided first-rate insight and suggestions regarding my work, and I feel very fortunate to have access to such excellent research intellect.

The U.C. Santa Barbara Geography Department has been an outstanding institution to develop my research interests as well as meet a wonderful group of people who have greatly enriched my life both personally and academically. Thanks to Violet Gray and David Lawson who helped get me started; Teresa Everett for keeping me (mostly) out of the administrative mire; my favorite officemate in the world: Chris MacFarland, I miss you man! And to all the regulars at Buffy night for lots of laughs, intelligent discussion and beer brewing fun. A special indebtedness goes to Noah Goldstein. How lucky am I to have such a good friend become my research collaborator? Thanks for all the great conversations. To you I owe my sanity.

Thanks to my family and friends for all the love, support and understanding you provide. A special shout out to The Contessa: my mentor and friend, what a wonderful Clarke-bonus you have been; and to Ann and Ken: so much of what is my life now would not have been possible without you.

Finally, my most deep felt appreciation to Jean Weekes. You have been a support and an inspiration to do more than I thought I could. Thank you.

Chapter 1

1 INTRODUCTION

Over the last century the presence of urbanization on the landscape has increased and intensified. Radically altering biotic, hydrologic, and land cover features; urban development has intense environmental impacts on local, regional and global scales. As a driving force in global change, the need to understand the dynamics of urban land use transitions and forecast urban growth patterns in an accurate and efficient manner is ever more pressing.

Urbanization is shaped by top down (environmental, political, socio-economic) factors as well as bottom up (personal, local, coincidental) choices. Describing the many drivers associated with urban change, and understanding their interrelatedness, is a massive and necessarily imperfect undertaking. Models generalize the intricacies of phenomena and offer an abstraction of the reality they represent. This abstraction, while not as precise as the reality, can offer an accurate, and more easily understood picture of a process. By applying models to the structure and complex dynamics of urbanization, primary spatial patterns and trends of growth can be simulated and a better understanding of the system as a whole may be achieved.

Urban researchers have used models to explain urban form since the early part of the 19th century when von Thunen published his classic model of agricultural location with respect to market places in 1826. The importance of von Thunen's observation of land use distribution was reiterated by Alonso's *Bid-Rent Theory* (1964) that

expanded upon von Thunen's theory by incorporating housing stock and land value to explain why particular land use patterns arise. Zipf's *Rank-Size Rule* applied to city size gave structure to the size distribution of settlements on the landscape. The internal structure and growth of cities centered on a central business district was examined in Burgess' *Central Zone Theory* (1925), Hoyt's *Sector Theory* (1939) and Harris and Ullman's *Multiple-nuclei Theory* (1945). While the models developed from these theories are useful in a general sense, their static nature disregards the dynamic processes of urban development.

The quantitative revolution in urban studies of the 1960's and 1970's led to the development of a diverse array of urban simulation models that explored the process of growth (Batty, 1981). A drawback of these models is that they were very complicated, and largely driven by technology rather than theory and failed to achieve the goals held out for successful urban models (Batty, 1981). Urban growth modeling was hindered by the central pursuit of explaining and modeling the origins of locational change (Liu, 2001).

The complex systems approach towards modeling suggests the multitude of interactions that take place on a micro scale form the basis of system-wide behavior. A methodology developed from complex systems is cellular automata (CA) simulation. First introduced by Von Neuman in 1966, CA presented the idea that a type of computing machine could not only reproduce itself, but could generate a machine of greater complexity than the original through the repeated application of a few simple rules. CA's can function upon a lattice, which make them explicitly spatial.

They operate through simple local rules, and are dynamic. In 1979 Tobler made the formal link between CAs and geographic modeling. In the last two decades CA have proven a useful tool for modeling dynamic urban systems (White et al., 1993; Papini and Rabino, 1997) yet literature regarding the calibration of these models remains sparse. Mathian et al., (2000) point out that various techniques of modeling dynamic spatial processes exist, but methods of calibration have lagged behind in development. As a way of simulating the dynamics of urban processes Clarke and Hoppen (1997) developed a modified cellular automaton of urban growth. Referring to the names of the input data used to initialize the model, *S*lope, *L*and-use, *E*xclusion, *U*rban, *T*ransportation, and *H*illshade, the model derives its name: SLEUTH. SLEUTH is a portable and scale independent model (Kramer, 1996) that has been applied in the San Francisco Bay Area (Clarke and Hoppen, 1997; Clarke et al., 1997), in the Washington-Baltimore region (Clarke and Gaydos, 1998), in the EPA designated Mid-Atlantic Integrated Assessment region (Candau and Clarke, 2000), and in the Middle Rio Grande Basin (Hester, 1999). Additionally, outside of the United States, SLEUTH has successfully been applied to the cities of Lisbon and Porto, Portugal (Silva and Clarke, forthcoming) and Mexico City, Mexico.

Santa Barbara, like most parts of California, is expecting an increase in population over at least the next thirty years. Area leadership has recognized that increased pressure to develop limited available lands could jeopardize the high quality of life enjoyed by Santa Barbara residents. Because of this, over the last several years an aggressive approach has been taken to involve a diverse cross section of the

community in discussing the future urban growth of the region and initiating planning efforts to protect the many amenities found in Santa Barbara, while maintaining a strong and growing economy. This strong interest in growth trends and community involvement has initiated the use of several types of urban models to explore and visualize future growth scenarios. These modeling efforts include the UGROW systems dynamic model, SCOPE systems dynamic model, UCIME integrated modeling effort, and SLEUTH.

The value of a model's predictions is only as good as the model's ability to be effectively calibrated (Clarke et al., 1997). Urban CA's are developed to represent the phenomena of urban development in a general way. Through the process of calibration, model parameters are refined to accurately represent an instance of that phenomena (e.g.; a particular city or region) (Silva, forthcoming). However, calibration of urban CA is rare, and testing of CA calibration methods has not been done. The need to address this knowledge gap regarding CA calibration is obvious. In an effort to better understand and define the efficacy of urban CA model calibration this research tests the sensitivity of the calibration methods of SLEUTH to scale and temporal input variations when applied to the Santa Barbara area. Lessons learned here will apply not only to SLEUTH, but may be transferred to CA calibration in general and inform the fields of urban and land use modeling, CA modeling and dynamic systems modeling.

The SLEUTH model is calibrated using historical data layers as controls. Clarke et al. (1997) described this methodology of robust calibration by way of visualization and

testing of alternative coefficient set solutions. In the implementation of this methodology, long-term calibrations that reach far back into the past are difficult and costly to assemble. This is due to the difficulty of generating complete data layers, and the inconsistency of data sources, classification and quality. Because of the increasing availability of remotely sensed data since the mid-sixties, shorter-term calibrations, utilizing data acquired from that period to the present, can provide more objective and consistent data classifications that will more reliably cover entire regions. In previous SLEUTH applications it has been assumed that the more historical data layers used, and the longer time period they represent, the better the calibration. This research, sponsored by the U.S. Geological Survey's Urban Dynamics project, challenges that assumption, and questions the importance of the temporal structure of calibration data. The null hypothesis of this research is: The duration and number of years used as controls for calibration of SLEUTH in the Santa Barbara study area will have no affect on the calibration results. In testing this hypothesis SLEUTH 3.0 will be applied to the Santa Barbara South Coast Region, the efficacy of long-term versus short-term calibration data for forecasting urban growth will be tested, the effectiveness of a set of SLEUTH calibration metrics for determining a best coefficient set will be considered, and the behavior of SLEUTH coefficients during calibration and forecasting will be illustrated.

Chapter 2

2 BACKGROUND

2.1 Urban Theory and Modeling

The use of models in scientific research is by no means new. This idea comes from the way people react with the real world (Liu, 2001). Virtually all systems in the real world are very complex. In order to explore the natural world, simplifications of real phenomena must be considered; the actual phenomena are too difficult to understand in their entirety. Through the development of a model a precise language is given to a theory about a system (Liu, 2001). Also, the validity of theory may be tested. This is especially advantageous in the social sciences, where controlled testing of theory using real world cases is largely impossible.

The most widespread use of models in urban geography was during the period of the quantitative revolution in Geography, which began in the late 1950's and continued until the late 1960's (Batty, 1981). This revolution was born out of necessity as well as convenience. Increasing car ownership during the 1940's and early 1950's led to the growing realization that cities with traditional physical forms could simply not cope with the "new mobility" (Batty, 1976). This led to the formation of transportation models in the late 1950's. Additionally, the development of digital computing machines provided a means of working with complex mathematical models which previously did not exist. Because planners viewed this group of models as providing "artificial laboratories" where otherwise impossible experiments on urban structure

could occur, a diverse array of styles, techniques and applications of urban models were developed during this period (Dyckman, 1963).

However, the emphasis of these mathematical models was on the modeling techniques rather than their theoretical representations, drawing criticism from many researchers in the field; most notably Lee's *Requiem for large-scale models* (1973). The theoretical shortcomings resulted in a substantial shift of attention in the late 1970's from using mathematical models to qualitative analysis in urban research. This emphasis on qualitative analysis continued until the late 1980's, when study on complex and open systems provided alternative ways to understand cities as evolutionary and complex systems (Allen, 1997). The development of geographic information systems and their integration with urban modeling has also facilitated the urban modeling with rich data sources and new techniques. These new developments have pushed the efforts of urban development modeling into a new era (Liu, 2001).

2.1.1 The von Thunen Model

Early in the 19th century von Thunen developed a model of land use that showed how market processes could determine how land uses were spatially distributed over a theoretical geographic area (Figure 2-1). It is easiest to explain this model in the context of agricultural land use. The model is based on the following limiting assumptions:

- The city is located centrally within an "Isolated State" which is self-sufficient and has no external influences.
- The Isolated State is surrounded by an unoccupied wilderness.

- The land of the State is completely flat and has no rivers or mountains to interrupt the terrain.
- The soil quality and climate are consistent throughout the State.
- Farmers in the Isolated State transport their own goods to market via oxcart, across land, directly to the central city. Therefore, there are no roads.
- Farmers act to maximize profits.

In an Isolated State with the above statements being true, von Thunen hypothesized that the agricultural land uses would segregate into a spatially hierarchic structure (Figure 2-1).

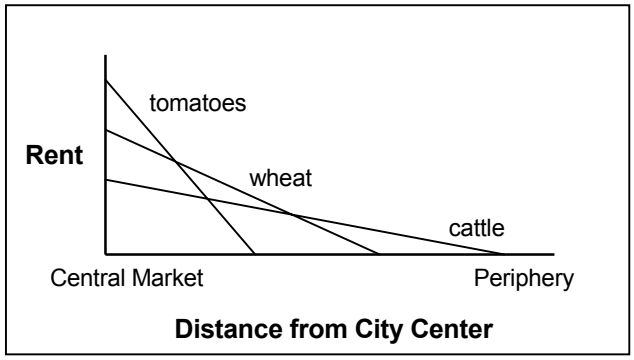

Figure 2-1: The von Thunen spatial organization of agricultural land uses.

Dairying and intensive farming occur closest to the city. Since vegetables, fruit, milk and other dairy products must get to market quickly, they would be produced close to the city. Since grains last longer than dairy products and fresh produce they can be located further from the city center. Ranching is located in the most peripheral areas surrounding the central city. Animals can be raised far from the city because they are

self-transporting. Animals can walk to the central city for sale or for butchering. Beyond the ranch land lies the unoccupied wilderness, which is too great a distance from the central city for any type of agricultural product.

Even though the von Thunen model is simplistic and created in a time before factories, highways, and even railroads, it is still an important model in geography. The Von Thunen model is an excellent illustration of the balance between land cost and transportation costs. As one gets closer to a city, the price of land increases. The farmers of the Isolated State balance the cost of transportation, land, and profit and produce the most cost-effective product for market.

2.1.2 Concentric Zone Theory

Proposed by E.W. Burgess (1926), Concentric Zone Theory evolved as an explanation of historical urban land use development in Chicago. Unlike the von Thunen approach, Burgess offers a descriptive rather than analytical account of these urban dynamics (Harvey, 1996). It is proposed that a city's land use may be classified as a series of concentric zones (Figure 2-2) and that the city grows by expanding these zones outward. Zone I is the central business district (CBD) and lies at the center of the city. Next is the multi-use transitioning Zone II with some migrant ghetto residences mixed with manufacturing. Zone III is characterized as a working class neighborhood. Amongst the factories are second-generation immigrants living in older homes with few amenities. Zone IV is occupied by middle class commuters.

The homes are newer and more spacious than those of Zone III. Zone V is for the upper class and is dominated by better quality housing and extensive amenities.

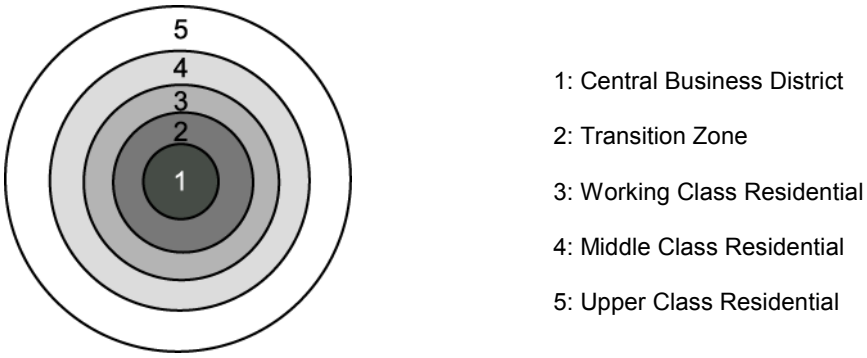

Figure 2-2: Concentric Zone Model

Like von Thunen, Burgess assumes a generalized geographic space and strict action space. Additionally, the important influence of topography and transportation are not considered, and the monocentric city is unreasonable for representing real land use patterns.

2.1.3 Central Place Theory

Central Place Theory was devised by geographer Walter Christaller (1933) in the course of studying settlement patterns in Southern Germany. In the flat landscape where Christaller lived, he observed that towns of a certain size were roughly equidistant. Through this observation Christaller examined and defined the functions of each settlement structure and the size of the hinterland. He found it possible to model each pattern of settlement locations using geometric shapes such as triangles and hexagons (Figure 2-3). The theory defines a central place as a settlement having a number of smaller towns at an equal distance away from it. These smaller towns use the central

places' shops and services often. The central place offers many more goods and services than a smaller town can. This framework bought about simple rules:

- The larger the settlement, the fewer there are of them.
- The less there are of a settlement, the larger the hinterland (or sphere of influence) of its services.

The conurbation below is the largest settlement and has a vast hinterland. It also has the largest amount of services. Because of this, such conurbations will seldom occur on the landscape. The cities, which have fewer services, are more plentiful and have much smaller hinterlands. This pattern continues in a hierarchical fashion to include smaller settlements of towns and villages. Each type of settlement will place itself in relation to the next larger settlement equidistance from settlements of the same size. In this way a hexagonal pattern of urban settlements are dispersed across the landscape.

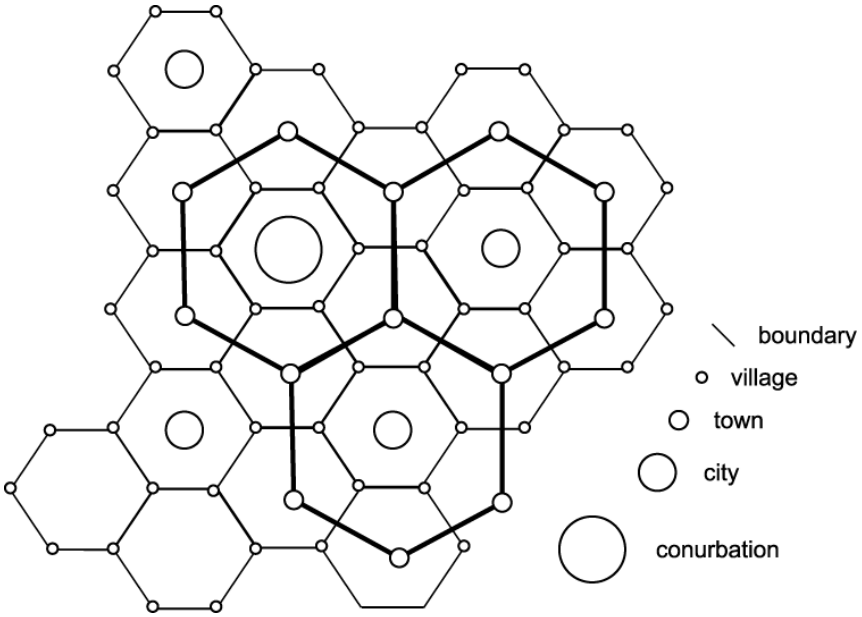

Figure 2-3: Christaller's central place model

2.1.4 Sector Theory

Hoyt (1939) was able to improve upon Burgess' Concentric Zone model by advancing the Sector Theory of urban land use. Based on residential land patterns in the United States, the location of business is referred to indirectly. " The model seeks to explain the tendency for various socio-economic groups to segregate in terms of their residential location decisions…The model suggests that, over time, high quality housing tends to expand outward from an urban center along the fastest travel routes" (Torrens, 2000). The sector model (Figure 2-4) considers direction in addition to distance as factors shaping residential allocation. Also, it recognizes that the CBD is not the only focal point of urban activity (Kivell, 1993).

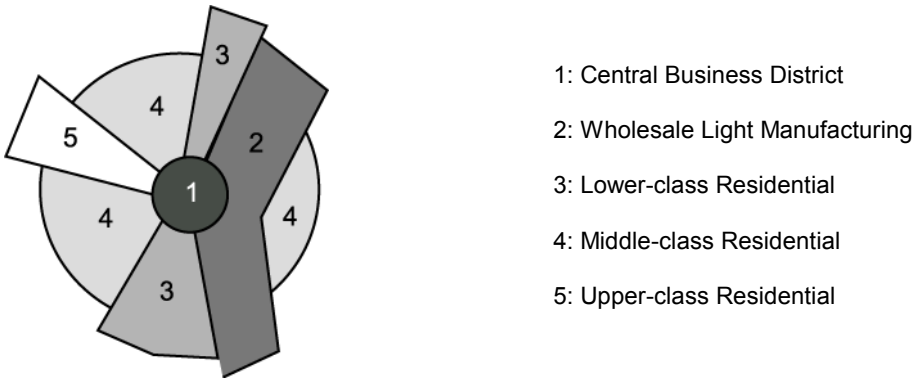

Figure 2-4: Sector Model

2.1.5 Multiple Nuclei Theory

Multiple Nuclei Theory, advanced by C. D. Harris and E. L. Ullman (1945) is based on the fact that many towns and nearly all large cities have many nuclei that serve as centers of agglomerative growth rather than a simple CBD around which all urban activity revolves (Figure 2-5). "Some of these nuclei are pre-existing settlements,

others arise from urbanization and external economies. Distinctive land-use zones develop because some activities repel each other; high-quality housing does not generally arise next to industrial areas, and other activities cannot afford the high costs of the most desirable locations. New industrial areas develop in suburban locations since they require easy access, and outlying business districts may develop for the same reason" (Mayhew, 1997). From this work, the idea of city spatial structure as predominantly cellular evolved. This theory surpassed previous attempts at explaining the spatial distribution of urban activity by acknowledging important influences such as topography, accessibility, and historical trends. Importantly, in recognizing the polycentric structure of cities multiple nuclei theory moves closer to explaining why urban spatial patterns emerge (Torrens, 2000) instead of only the how.

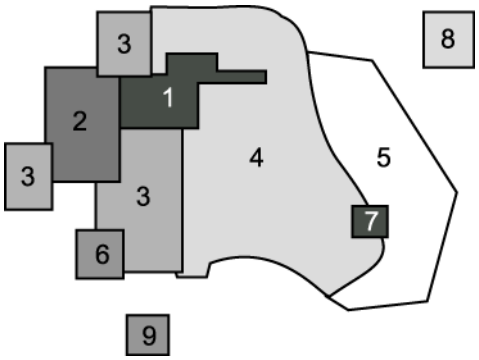

Figure 2-5: Multiple-nuclei model

1: Central Business District
2: Wholesale Light Manufacturing
3: Lower-class Residential
4: Middle-class Residential
5: Upper-class Residential
6: Heavy Manufacturing
7: Outlying Business District
8: Residential Suburb
9: Industrial Suburb

2.1.6 Zipf's Rank-Size Law

First explained by (Zipf, 1949) the rank-size law of cities has been one of the most conspicuous empirical facts in economics, or in the social sciences generally (Gabiax, 1999). This law links, through a linear relationship, cities' frequency of occurrence to

their unit size. According to Zipf, if the population of a town is multiplied by its rank, the sum will equal the population of the highest ranked city.

> *To visualize Zipf's law, we take a country (for instance the United States), and order the cities by population: No. 1 is New York, No. 2 is Los Angeles, etc. When we draw a graph; on the* y*-axis we place the log of the rank (N.Y. has log rank ln 1, L.A. log rank ln 2), and on the x-axis the log of the population of the corresponding city (which will be called the "size" of the city). We take, like (Krugman, 1996), the 135 American metropolitan areas listed in the Statistical Abstract of the United States for 1991. (Gabiax, 1999)*

The result of such a plot is a strait line with a slope of –1 and an r^2 of nearly 1.0. What is so surprising about this result is there is no top-down policy that would cause it to be so. The pattern is emergent. Further, similar results can be achieved for most countries in the modern period (Rosen and Resnick, 1980), for other periods in U.S. history (Zipf, 1949; Rosen and Resnick, 1980; Krugman, 1996; Krugman, 1996), as well as in other countries for different periods: India in 1911 (Zipf, 1949), and China in the mid-nineteenth century (Rozman, 1990). (It must be noted, however, that important examples of exceptions to the rule do exist: London, U.K., Paris, France, and Tokyo, Japan among others.)

Many attempts have been made to explain Zipf's law, but each has had important inadequacies (Gabiax, 1999). The debate of its causes is beyond the scope of this work, but a recent explanation has been offered by Gabiax (1999) who proposes "Zipf's law derives from Gibrat's law, where Gibrat's law means that the growth

process is independent of size (Gabiax, 1999)". A comprehensive review of this literature is given by Carroll (1982). What is important to this discussion is that Zipf's law shows that the distribution of cities maintains a linear relationship between city size (measured by population) and rank, and this relationship is true across scales and time. It is possible to modify this theory to a spatial metric by redefining the unit of measure as area of urban cluster (where *urban cluster* is defined as the amount of land contained within a contiguous agglomeration of urban land use) instead of city population. The cluster size could then be plotted against its rank to test how well the spatial distribution of the city follows the rank size rule.

2.1.7 Bid-Rent Theory

Taking the von Thunen model one step farther, the bid-rent theory popularized by (Alonso, 1964) offers an explanation of the spatial distribution that von Thunen described. Since transport costs rise with distance from the market, rents generally tend to fall correspondingly, but different forms of land use (retail, service, industrial, housing, or agricultural) generate different bid-rent curves (Figure 2-6). The urban land user seeks central locations, but is willing to accept a location further from the city center if rents are lower in compensation. The use that can extract the greatest return from a site will be the successful bidder. Illustrating bid-rent theory in an alteration of von Thunen's model, (Alonso, 1964) in a study of housing, compared the quantity of land needed, and variations in the amount of income used on land, transport costs, and on all goods and services. If the amount of goods and services is held constant, the price of land should decrease with increasing distance from the center and a pattern of housing stock will emerge. The quantity of land that may be

bought should increase with distance from the center, but commuting costs will rise with distance from the center. From this basic principle Alonso illustrated how the well-off will choose the amenities of lower density housing at the edge of the city, and pay the price of commuting over distance, while the poor remain in high density residences near the city center. Each household represents a balance between land, goods, and accessibility to the workplace (Mayhew, 1997).

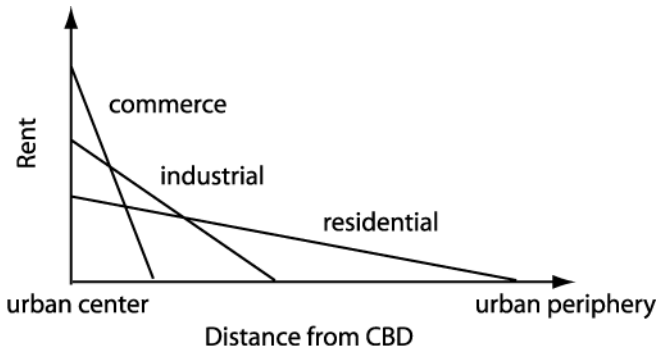

Figure 2-6: The Alonso model of housing stock based on bid-rent

The assumptions of von Thunen and Alonso present a greatly simplified geographic and decision space that is far from reality. However, their models do reflect some aspects of dynamic urban morphology and the bid-rent curves describe how these patterns emerge.

Hedonic price models, a variant of bid-rent models, have been more effective in putting into practice some of the factors that weigh into the bid-rent calculation. Hedonic price models reduce real estate values into their fundamental elements, each of which has an associated value thus enabling extended disaggregation. Two main factors trouble the application of the hedonic model: They are weakened by the

reliance upon market value for formulating hypotheses about urban dynamics, and market value data may be difficult to acquire, especially over multiple time periods, due to privacy concerns (Torrens, 2000).

2.1.8 Theory of automata

The above theories are based primarily on empirical observation. Many hypotheses on how these urban structures arise (such as equilibrium between forces of concentration and dispersion, agglomeration of economies, or maximization of social interaction) propose a constraint that controls system evolution. However, evidence to support such universal constraints has not been demonstrated. Rather, most convincing interpretations see macro-scale pattern as arising from the micro-scale interactions of the components that make up the system. Pioneers in this approach came not from the field of urban research but physics and mathematics.

In the 1930's Alan Turing proposed a hypothetical machine with limited specifications and ranges of action that was capable of computing anything that could be computed. Using simple rules and given an appropriate initial state, this machine, or automaton, could evolve into a replica of itself and have the ability to produce further copies. Hypothetically, this "Universal Turing Machine" was the one meta-machine needed to build any system. "(Turing) figured out that mathematicians, unlike carpenters, only needed to have one tool in their toolbox, if it were the right sort of tool" (Stephenson, 1999). In the 1940's, inspired by Turing's work, John von Nuemann (originator of game theory and pioneer in set theory and quantum mechanics) in collaboration with renowned mathematician Standislav Ulam (who worked on Monte Carlo simulation and the Manhattan Project atomic bomb) developed Cellular Automata (CA) as a

framework for investigating the logical underpinnings of life. "They were interested in exploring whether the self-reproducing features of biological automata could be reduced to purely mathematical functions – whether the forces governing reproduction could be reduced to logical rules" (Torrens, 2000).

Von Nuemann (1966) proposed his new "theory of automata" as a coherent body of concepts and principles concerning:

1. the structure and organization of both natural and artificial systems.
2. the role of language and information in such systems.
3. the programming and control of such systems.

An actualization of this theory would be the creation of automata containing a Turing machine that is able to compute anything that is computable. This theory was expressed in Conway's CA *Game of Life* popularized by Gardner in 1970.

A formal link between CA and geographic phenomena was made by Tobler's *Cellular Geography* (1979) where the implicitly spatial nature of the transition rules made CA "the geographical type of model par excellence" (Couclelis, 1985). In 1985 Helen Couclelis presented a simple cellular modeling framework for land use based on discrete structure theory. Also during the 1980's and early 1990's much work was done identifying urban systems as fractal forms and complex systems (Burroughs, 1981; Batty and Longley, 1986; Batty and Longley, 1987; Batty and Longley, 1988; Batty et al., 1989; Longley et al., 1990; Batty, 1991; White and Engelen, 1993; White et al., 1993). In the following section, the complex systems approach to urban modeling, especially through the methodology of CA, is explored more fully.

2.2 Complexity and the Cellular Automata Approach

Complex systems approaches suggest the multitude of interactions that take place on a large-scale, or individual level, form the basis of system-wide, or aggregate, behavior. In emergent systems, which are key to the idea of complexity, a small number of simple rules applied locally can result in a system that is surprisingly complex but not necessarily chaotic (Torrens, 2000). An underlying structure can usually be discovered. What is important about this approach is the power of the local agent, without reference to any system-wide driver, to generate organized, recognizable, macro-scale features that change over time.

A problem faced by geographers in trying to model human systems is aggregating from the actions of an individual to the dynamics of the whole. This is especially difficult when the local-scale actions are interdependent. Information cannot simply be aggregated to the small-scale generalization of system dynamics. Instead, "an understanding of the *interactive* dynamics that link local-scale and smaller-scale phenomena" (Torrens, 2000) needs to be pursued. Essentially, in emergent systems, the whole is not a sum of its parts, but a result of the parts' dynamics. A synthetic approach, bringing parts together to form an interactive whole, as opposed to a reductionism approach, which separates the whole into its parts, is becoming more popular among researchers studying complex, dynamic systems. A way to understand the interactions of a system is by applying simple rules to the components, and observing how these rules affect the behavior of the individual agents over time, until macro scale processes emerge. Learning occurs by bringing the pieces together, rather than dividing them into parts.

Complexity has much to offer in possibilities, but it is not without its critics, even from within the very walls of the Santa Fe Institute where the potentials of complexity were first touted. Criticisms from Jack D. Cowan, a mathematical biologist from the University of Chicago who helped to found the institute, were quoted in Horgan (1995). First among these criticisms is the reminiscence "syndrome" suffered by those advocating computational simulation results of complex systems. This condition calls attention to how a simulation is reminiscent of a biological or physical phenomenon. "They (supporters of complexity) jump in right away as if it's a decent model for the phenomenon (because of reminiscence), and usually it's just got some accidental features that make it look like something" Cowan in (Horgan, 1995). Reminiscence may in fact only be a result of coincidence, without necessitating the discovery of a greater understanding of the phenomena being modeled. Also, modification of complexity formalisms (i.e.; modification of the simple cellular automata) to better simulate a process might produce more relevant results, but runs the risk of creating a model so complex, that the simplicity and transparency of the simple rules are lost (Couclelis, 1985; Horgan, 1995; Couclelis, 1997). Additionally, while computational models are necessarily rule based, and thus lend themselves to the synthetic approach, there is no reason to believe that all phenomena in the natural world is rule-based and should be modeled as such (Casti, 1997).

The proponents of complexity have not delivered on everything that was promised, not the least of which is an all encompassing "unified theory" of complex systems. Some even admit that "we are not even close" to its development (Casti, 1997). But

these criticisms should not be enough to cause the dismissal of the complex system approach. One thing that is evident is complex systems do not lend themselves to simple scientific examination (Horgan, 1995). The field still has much to offer in the understanding of interactive and dynamic systems. Cities have several qualities that ally themselves with complexity definitions. It must be acknowledged however that not all processes of the urban environment will be appropriate for this type of examination.

A first application of complexity methods was introduced from the discipline of computer science. John Von Neuman (1966) presented the idea that a type of computing machine could not only reproduce itself, but could generate a machine of greater complexity than the original. This concept was expressed in the form of a CA. The best-known example of a CA is the *Game of Life* developed by John Conway (Gardener, 1972). The formalism of the CA has a few basic tenets: The area of the CA, or "game space" is a regular tessellation of cells. A finite number of discrete cell states are defined, and a cell may exist in only one state at a discrete period of time (t). Transition rules, which applied uniformly across the game space relate a cell's state to that of its immediate neighbors at time (t) to determine its state at ($t+1$). Cell states are updated synchronously to the next time period. In the transitions process, each cell acts within the system as an independent agent. Its condition is dictated not through outside determinants, but rather, as a result of the current state of a cell and the state of its neighbors. Further, since all transitions are impressed upon the game space at the same time, change is both spatially and temporally correlated. It was discovered

that, depending on the configuration of the initial conditions, complex spatial patterns could emerge though repeatedly applying simple behavior rules to the grid. "These models demonstrate with powerful immediacy the generally unpredictable dynamic relationship between local events and global structure" (Couclelis, 1985).

CA have several traits that make them seem natural tools for simulating urban dynamics. Cells can represent many of the elements that make up an urban system: built structures, parcels, census units, automobiles, traffic analysis zones, etc. Similarly, cell states may be assigned for the attributes of an urban area. A simple example is the binary attributes of urban/non-urban. Various others can be used: population density, land use, land cover, etc. The inherently spatial qualities of CA models also make them uniquely qualified for applications to geographic phenomena. Neighborhoods provide spatial context to influence transitions at discrete locations. Change at each cell has a spatial and temporal autocorrelation that imitates the interactive properties of urban spatial settlement decisions. The transition rules can be created to mirror how real urban systems operate, and then coded as algorithms within the simulation (Torrens, 2000). By placing urban elements as attributed cells within a dynamic CA, urban processes may be studied as a synthetic system.

Many good links can be found to attach urban dynamics to complexity and CA simulation. Choices made by individuals at the local-scale are interdependent and can be aggregated into large-scale, or global phenomena (Nagel et al., 1996). Additionally, the physical form of the city exhibits several of the signature characteristics of complex systems including fractal dimensionality and self-similarity across scales,

emergence, and self-organization (Batty and Longley, 1987; Longley et al., 1990; Batty, 1991; Torrens, 2000). As stated above, CA are advantageous as models of urban systems because of their dynamic and spatially explicit qualities, and expression of complex system characteristics. Additionally, the lattice game space utilized by CA facilitates integration with GIS and remotely sensed data. Also, the CA lattice format is an easily visualized medium that can be compiled into animation for dynamic presentation of simulated behavior.

Informal urban modeling in a cellular space was first demonstrated by Tobler (1970), who eventually formalized the approach in his definition of cellular geography (Tobler, 1979). Examples of applying CA to various urban systems abound. In recent years CA models have been used to study urban and metropolitan growth (Clarke and Hoppen, 1997; Sembolini, 1997; White and Engelen, 1997; Clarke and Gaydos, 1998; Batty and Xie, 1999; Li and Yeh, 2000; Ward et al., 2000). The dynamics of urban and other land cover transitions due to urban development have been explored (Cecchini, 1996; White and Engelen, 1997; White et al., 1997; Webster and Wu, 1999; Webster and Wu, 1999; Candau et al., 2000). A specific systems modeling approach towards cities and regions has been applied (Portugali and Benenson, 1995; Sanders et al., 1997; Sembolini, 1997; White and Engelen, 2000). International social-spatial migration patterns (Sembolini, 1997; Portugali, 2000) and the competitive behavior of location optimization (Benati, 1997) have been simulated. Polycentric (Wu, 1998) urban growth and its stability have been explored. And by using CA to recreate

regional urban growth, a comparison of historical growth trends for different cities has been accomplished (Silva and Clarke, forthcoming).

Most models require a relaxing of the formal CA structure in order to more realistically represent real world phenomena. A few interesting examples of the CA variations include: an expanded, 112 cell, neighborhood (White and Engelen, 1993), non-uniform lattice conditions (Clarke and Hoppen, 1997; White and Engelen, 1997; Clarke and Gaydos, 1998), asynchronous transition rules (White and Engelen, 1993; White and Engelen, 1997; Wu, 1999), and self-modifying transition rules (Clarke and Hoppen, 1997). There are some processes of urbanization, such as planned zoning and transportation infrastructure, which do not occur at local scales. The formal CA lacks the allowance of action at a distance (Batty et al., 1997), but instances of allowing distance influence also exist (Clarke and Hoppen, 1997; White et al., 1997; Ward et al., 2000). Thus far in CA development multi-dimensional models have been avoided, and a preponderance of urban CA models remain in two-dimensional space, in spite of the fact that this restriction greatly limits the CA's applicability to the urban environment. This is primarily a result of the coding and computational difficulties involved in leaving the flat plane. A notable exception to this is found in Sembolini (2000). Similarly, because of source data format and coding difficulties, most urban CA have operated on a lattice of regular squares. An exception to this is Sanders' et al. hexagonal cells (Sanders et al., 1997).

One of the attractions of CA is that by observing actions at the local level, something can be learned about the dynamics of the urban system. However, as the formalisms

of the CA are relaxed, the behavior resulting from the growth rules becomes more complex, generating the possible paradox: While we might be able to simulate a simplified urban phenomena using a modified CA, will we be able to derive any knowledge about the system itself from the application, or will the modeled behaviors be too complicated? Also, the dependence upon action at a local level assumes a closed system, which cities are not. The evolution of an urban system's configuration is a process influenced by a large number of forces both natural to the environment, such as wildfires (Goldstein, 2001) and floods, and imposed by human design, such as systems of transportation and zoning policies or pressures from economic boom or depression. These affects may be global or discrete and act outside of local interaction. At present, there is no clear way to solve these issues. Couclelis (1997) points out that while the application of CA to urban dynamics seems natural and intuitive, that in itself is not a justification for their use, and in fact their most appropriate use may be as a metaphor of urban systems rather than a model. O'Sullivan and Torrens (2000) offers, "the important criteria for such operational models must be the extent to which model behavior is theoretically plausible and therefore believable."

2.3 Calibration of Cellular Urban Models

The goal of urban models is to simulate some aspect of the urban system. If a model is developed for a specific city or region its applicability to another location is likely to be impossible. If this is the case, the model's use is quite limited. Alternatively, if a model simulates characteristics that are general to the process of urbanization, such as edge growth and infilling, but allows for adjustment to more realistically portray a

specific instance of that process, the usefulness of the model is greatly increased. Such a general-purpose model may be applied to multiple cities and is refined for each new application through the process of calibration (Silva, forthcoming).

Parameters affect how a model simulation evolves. The objective of model calibration is to determine the numerical values of the model parameters (Giudici, 2001). Examples of urban CA models are plentiful, but methods of calibration remain sparse. This is due in part to the fact that the computational requirements of CA calibration are considerable while forecasts are generated relatively easily. Also, CA models are difficult to calibrate because metrics that comprehensively describe the dynamic process of urbanization do not exist. Clarke et al. (1997) proposed using several spatial and statistical metrics to quantify how well simulated urban extent matched historical data gathered from maps and remotely sensed data for several periods in time. The model is initialized at some date in the past and then used to "predict" current urban land use configuration. This methodology has been used successfully in several applications ((Kramer, 1996; Clarke and Hoppen, 1997; Clarke and Gaydos, 1998; Candau and Clarke, 2000; Silva and Clarke, forthcoming), and others) and is described in detail in section 3.2.3.

3 THE SLEUTH LAND COVER MODEL

Several terms specific to SLEUTH will be used in this and the following sections. To encourage clarity, the table below lists what group these terms fall into. Also, a type-font convention for each group is shown in this table and is used throughout the remaining text to identify these terms. Most recurring terms are defined in the glossary. Equation variables are not listed here, but will be identified with ***italicized Times New Roman*** font in the text.

Growth rules	Growth coefficients	*CONSTANTS*	`ASCII files`

spontaneous
new spreading center
edge
road-influenced
	Dispersion
	breed
	spread
	slope-resistance
	road-gravity
		CRITICAL_HIGH
		CRITICAL_LOW
		CRITICAL_SLOPE
		BOOM
		BUST
			`avg.log`
			`controlstats.log`
			`scenario.file`

3.1 Modified Cellular Automaton Model

SLEUTH is a modified CA model of urban extent originally described in (Clarke and Hoppen, 1997), and is discussed here as its most recent version: SLEUTHv3.0. SLEUTHv3.0 is a C programming language model optimized and restructured by the Environmental Protection Agency to run in an optional parallel computing environment. The urban growth model is the main component of SLEUTH and the subject of this work. The Deltatron land use model is the second component, and it is implemented as an optional add-in that is tightly coupled with, and driven by,

simulated urban growth. Complete documentation and downloadable code may be found at the Project Gigalopolis website: www.ncgia.ucsb.edu/projects/gig.

In an effort to more realistically portray urban growth, some of the formalisms of simple CA have been relaxed. As with a standard CA, SLEUTH begins with an initial set of conditions, after that a set of transition rules is applied. The initial conditions are defined by input image data. The input data serve as layers of information that create a non-homogenous cellular space and influence cell transition suitability. The application of transition rules is affected by growth parameters. These coefficient values may be altered at the end of each time step by self-modification constants. SLEUTH's self-modification behavior emulates increases and decreases in urban growth trends, simulating rapid, system-wide "boom" and "bust" states.

3.1.1 Initial Conditions

Raster data defines the initial state of the CA simulation space. SLEUTH uses several types of geographic data to generate an initial system configuration and transition suitability surface:

3.1.1.1 Slope

Topography, in general terms, creates the most basic definition of area available for urban development. Because of ease of development, flat expanses are the easiest to build upon. Lands get less hospitable as slope increases, and eventually become impossible to develop due to structural infeasibility. The point where structures are no longer built due to slope constraints is defined as *CRITICAL_SLOPE*.

3.1.1.2 Land-use

Land-use classes additional to urban may be modeled in SLEUTH. This is an optional input, and was not utilized in this application.

3.1.1.3 Exclusion

Areas not available to urbanization are included in the exclusion layer. Water bodies, parklands, and national forest are all good examples of commonly excluded land-use types. The exclusion layer is not necessarily binary and may include levels, or probabilities, of growth resistance.

3.1.1.4 Urban

This is a binary classification: urban or non-urban. How "urban" is defined is application dependent. Methods used in the past include digitizing city maps and aerial photographs, thresholding remotely sensed images or block densities from census data. For calibration, at least four urban layers are required in order to calculate best-fit statistics.

3.1.1.5 Transportation

A transportation network can have an important role in a city's developing structure. Due to increased accessibility, urban corridors tend to reach out from the city core along modes of transportation. The transportation infrastructure expands with city growth. To include the dynamic effect of transportation in calibration, several road layers that change over time are desirable. SLEUTH is initialized with the earliest road layer. As growth cycles, or "time", pass and the date for a more recent road layer is reached, the new layer is read in and development proceeds. The

roads are not necessarily binary, but may be weighted to simulate one section of road's greater attractiveness to urbanization relative to another section of road.

3.1.1.6 Hillshade

A grayscale background image gives context to the spatial data generated by the model. It is useful for describing location and scale as well as topography. This layer is not an active input for model simulation, but can greatly assist the visual examination and analysis of model output image.

3.1.2 Growth Rules

The dynamics of urban growth are expressed by four rules: *spontaneous, new spreading center, edge*, and *road-influenced* Candau et al. (2000). *Spontaneous growth* simulates the occurrence of a new urban settlement on the landscape without necessary relation to preexisting infrastructure. *New spreading center growth* controls the likelihood that one of the newly established *spontaneous growth* settlements will become a center for continued growth. *Edge growth* models outward growth from the city edge as well as urban in filling. *Road-influenced growth* generates spreading centers next to routes of transportation and simulates the tendency for new growth to follow lines of transportation. These growth rules occur sequentially, and the cell state is updated after the application of each rule across the entire space. For a full discussion of the SLEUTH growth dynamics see (Candau et al., 2000).

3.1.3 Growth Coefficients

Five coefficients, or parameters, affect how the growth rules are applied. Each coefficient may be an integer between 0 and 100. Comparing simulated land cover change to a study area's historical data and calculating linear regression, goodness-of-

fit scores (r^2) calibrate these values. The descriptions below outline the five coefficient values, which transition rules they affect, and how the applied values are derived from the coefficients.

3.1.3.1 Dispersion Coefficient

The dispersion coefficient (in previous literature referred to as diffusion coefficient) controls the number of times a pixel will be randomly selected for possible urbanization during *spontaneous growth*.

An applied value is derived from the dispersion coefficient by:

$$dispersion\_value = (dispersion\_coefficient * 0.005) * \sqrt{nrows^2 + ncols^2}$$

so that *dispersion_value* at its maximum (where dispersion_coefficient is defined as 100) will be 50% of the image diagonal.

The dispersion_value is then applied to spontaneous growth by:

```
for ( k = 0;  k < dispersion_value;  k++ )  {
  select pixel (i,j) at random;
  try to urbanize (i,j);
}
```

The dispersion coefficient also controls how many "steps", or pixels, make up a random walk along the transportation network on a road trip as part of *road-influenced growth*.

The dispersion coefficient is applied to *road-influenced growth* by:

$$run\_value = dispersion\_coefficient$$

where *run_value* is the maximum number of steps traveled along the road network.

3.1.3.2 Breed Coefficient

The breed coefficient determines the probability of a pixel urbanized by *spontaneous growth* becoming a *new spreading center*.

The breed coefficient is applied to *new spreading center growth* by:

Given: a newly urbanized *spontaneous growth pixel* (*i,j*).

```
if ( random_number < breed_coefficient ) {
   attempt to urbanize two neighbors*;
}
```

The breed coefficient also determines the number of times a road trip will be taken during *road-influenced growth*.

The breed coefficient is applied to *road-influenced growth* by:

```
for ( k = 0;  k <= breed_coefficient;  k++  ) {
   head off on a road trip;
}
```

3.1.3.3 Spread Coefficient

The spread coefficient determines the probability that any pixel that is part of a spreading center (a cluster of pixels of three or more in a nine cell neighborhood) will generate an additional urban pixel in its neighborhood.

The spread coefficient is applied to *edge growth* by:

```
if ( random_number < spread_coefficient) {
  attempt to urbanize neighboring pixel;
}
```

3.1.3.4 Slope Coefficient

---

* In this growth rule algorithm two neighbors are urbanized because the following growth rule, *edge growth*, will look for urban clusters of three or more, and increase the number of urban pixels of such a cluster in subsequent growth cycles. In this way some urban clusters (<3) will

The slope coefficient affects all growth rules in the same way. When a location is being tested for suitability of urbanization, the slope at that location is considered.

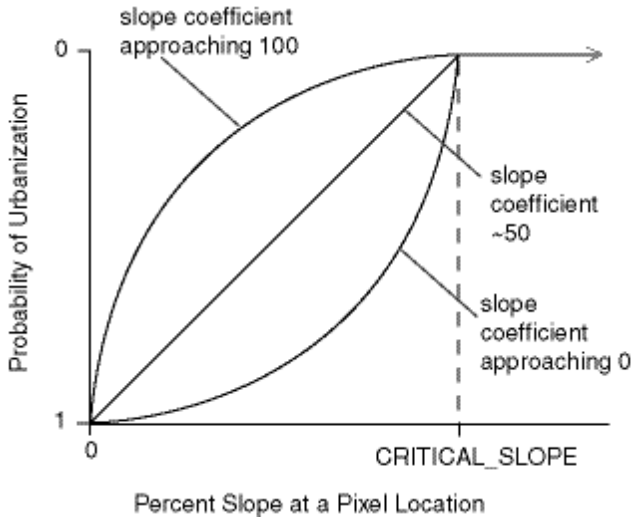

Figure 3-1: Affect of the slope resistance coefficient

Instead of enforcing a simple linear relationship between the percent of slope and urban development, the slope coefficient acts as a multiplier. If the slope coefficient is high, increasingly steeper slopes are more likely to fail the slope test. As the slope coefficient gets closer to zero, an increase in local slope has less affect on the likelihood of urbanization (Figure 3-1).

Creating a lookup table that relates actual slope values to slope coefficient-influenced probabilities enforces this dynamic relationship.

---

remain small, non-agglomerating elements while others (>=2) will become new spreading centers.

The slope coefficient is used to calculate slope weights by first calculating:

$$ex = slope\_coefficient / MAX\_SLOPE\_RESISTANCE / 2.0 \text{ co}$$

where *MAX_SLOPE_RESISTANCE* set to 100 and ex is an influencing exponent value. Using the ex value, a lookup table is then built by:

```
for ( i = 0; i < lookup table size; i++ ) {
  if ( i < critical_slope ) {
     val = (CRITICAL_SLOPE – i) / CRITICAL_SLOPE
    lookup_table[i] = 1.0 - val^ex;
  } else {
     lookup_table[i] = 1.0;
  }
}
```

3.1.3.5 Road Gravity Coefficient

During *road-influenced growth* the maximum search distance from a pixel selected for a road trip for a road pixel is determined as some proportion of the image dimensions. The applied value is derived from the road gravity coefficient (*rg_coef*) by:

$$rg\_value = (rg\_coef / MAX\_ROAD\_VALUE) * (nrows + ncols / 16.0)$$

where *MAX_ROAD_VALUE* is defined as 100, and nrows and ncols are the row and column counts respectively. So *rg_value* at its maximum (when *rg_coef* equals 100) will be 1/16 of the image dimensions. If the *rg_coef* is less than 100, then the *rg_value* will be some proportion less than 1/16 of the image dimensions.

Rg_value is then applied to road-influenced growth by:

$$\max\_search\_index = 4 * rg\_value * (1 + rg\_value)$$

where *rg_value* defines the maximum number of neighborhoods from the selected urban pixel to search for a road.

The first neighborhood (*rg_value* == 1) is made up of the selected urban pixel's adjacent 8 cells. The second neighborhood (*rg_value* == 2) would be the 16 pixels outwardly adjacent to the first neighborhood, etc. In this way the outward search for a road will continue until (a) a road is found, or (b) the search distance is greater than *MAX_SEARCH_INDEX*.

3.1.4 Self-Modification

A growth cycle is the basic unit of SLEUTH execution. It begins by setting each of the coefficients to a unique value. Each of the growth rules is then applied to the raster data. Finally, the resulting growth rate is evaluated. If the growth rate exceeds or falls short of limit values, model self-modification is applied. Self-modification will slightly alter the coefficient values to simulate accelerated or depressed growth that is related with system-wide boom and bust conditions in urban development.

To apply self-modification, the first step is to determine if the system is in a growth or stable period of development. A "boom" state occurs if the growth rate exceeds the *CRITICAL_HIGH* value and indicates a period of accelerating growth. Each of the coefficients is increased to encourage the continuation of this trend. A "bust" state occurs when the growth rate is less than the *CRITICAL_LOW*. In such an instance the coefficients will be lowered in order to decrease the rate of growth throughout the system.

The algorithm used to apply self-modification to the coefficients is given below:

Given:

$$growth\_rate = number\_growth\_pixels / total\_number\_urban\_pixels * 100$$

$$percent\_urban = \begin{pmatrix} 100 * (total\_number\_urban\_pixels + road\_pixels) / \\ (total\_number\_pixels - road\_pixels - excluded\_pixels) \end{pmatrix}$$

where *number_growth_pixels* is the number of newly urbanized pixels from the current growth cycle, *total_number_urban_pixels* is the amount of urban pixels from the current and previous growth cycle, *road_pixels* is the number of road pixels used for the current growth cycle, and *excluded_pixels* is the number of pixels in the exclusion layer with an absolute exclusion value.

if (*growth_rate* > *CRITICAL_HIGH*) {
$slope\_res = slope\_res - (percent\_urban * SLOPE\_SENSITIVITY)$
$road\_grav = road\_grav + (percent\_urban * ROAD\_GRAV\_SENSITIVITY)$
    if (dispersion < *MAX*) {
  dispersion = dispersion * *BOOM*;
  breed = breed * *BOOM*;
  spread = spread * *BOOM*;
  }
}

where *CRITICAL_HIGH* is the growth rate threshold above which a boom state exists for the system. Slope_res, road_grav, dispersion, breed, and spread represent the coefficient values slope_resistence, road_gravity, dispersion, breed and spread respectively. *SLOPE_SENSITIVITY, ROAD_GRAV_SENSITIVITY,* and *BOOM* (as well as *BUST* used in the bust state) are used to modify the coefficient values and are defined in the application `scenario` file. *MAX* is the maximum value of a coefficient.

if (growth_rate < *CRITICAL_LOW*) {
$slope\_res = slope\_res + (percent\_urban * SLOPE\_SENSITIVITY)$
$road\_grav = road\_grav - (percent\_urban * ROAD\_GRAV\_SENSITIVITY)$
    if (dispersion > 0) {
    disperson = dispersion * *BUST*;
    breed = breed * *BUST*;

```
    spread = spread * BUST;
  }
}
```

where *CRITICAL_LOW* is the lower limit for *growth_rate*, below which the system enters a bust state.

3.2 SLEUTH Calibration Approach

3.2.1 Fitting Historical Data

A major tenet of SLEUTH application is: by calibrating how a region has changed in the past, a reasonable forecast of future change can be made (Clarke et al., 1997). Following this assumption, the model is calibrated by fitting simulated data to historical spatial data collected from maps, aerial photography or other remotely sensed data. Input requirements are discussed in detail in Section 3.1.1. SLEUTH is initialized with the earliest data (signifying the date furthest in the past) and growth cycles are generated. It is assumed that one growth cycle represents one year. As growth cycles complete, "time" passes. Dates where historical data exist are referred to as control years. When a completed cycle has a corresponding control year, an image of simulated data is produced and several metrics of urban form (see Section 5.2.2) are measured and stored in memory.

3.2.2 Monte Carlo Averaging

Due to the high amount of randomness present in each growth cycle, growth simulations are generated in Monte Carlo fashion to bring a greater amount of stability to modeled results. Monte Carlo averaging reduces dependence upon initial conditions and stochasticity. When a coefficient set has completed a defined number of Monte Carlo simulations, the metric values stored to memory are summed and

divided by the number of Monte Carlo iterations. These averaged values are then compared to the control data metrics and linear regression, best-fit statistics are calculated.

3.2.3 SLEUTH Brute Force Calibration

SLEUTH utilizes five coefficients that may range independently between zero and 100. This poses a large set of possible solutions and a daunting number of computer processing unit (CPU) cycles required to explore the multidimensional coefficient space. As a way to reduce the number of solution sets but still search the range of solutions, the methodology of brute force calibration has been utilized to derive parameter values. Instead of executing every permutation of possible coefficient sets, each parameter range is examined in increments. For example, the range {0-100} may be stepped through in increments of 25 resulting in the values {0, 25, 50, 75, 100} or 5^5 simulations being implemented in order to cover the range. In this way, the model may be calibrated to the data in steps, successively narrowing the range of coefficient values. Generally, this process is accomplished in three phases here referred to as *coarse*, *fine* and *final*.

3.2.3.1 Coarse Phase

In the initial, coarse phase of calibration, the entire range (0 – 100) of the five coefficients is explored using large increments (e.g.; for each coefficient, value = {0, 25, 50, 75, 100}) and a small number (4) of Monte Carlo iterations are used.

3.2.3.2 Fine Phase

Using the best-fit values found in the `control_stats.log` file produced in the coarse calibration phase, the range of possible coefficient values is narrowed.

Ideally, the ranges will be narrowed so that increments of 5 - 10 may be used while still only using about 5-6 values per coefficient (e.g.; for a single coefficient, value = {25, 30, 35, 40, 45, 50}) and a larger number of Monte Carlo iterations are used (6).

3.2.3.3 Final Phase

Using the best-fit values found in the `control_stats.log` file produced in the fine calibration phase, the range of possible coefficient values is narrowed. Ideally, the ranges will be narrowed so that increments of 1 - 3 may be used while still only using about 5-6 values per coefficient (e.g.; for a single coefficient, value = {4, 6, 8, 10, 12}) and a larger number of Monte Carlo iterations are used (8).

3.2.3.4 Calibration Scalability Experiment

Even with the employment of the brute force methodology, the computational requirements of running SLEUTH may still be quite large due to the number of historical years being simulated and image size of the input data. As a way to reduce this computational overhead, and maintaining the absolute scalability of the model, previous model applications have used resampled, or coarsened data in the initial phases of calibration to further reduce the CPU cycles required.

In order to test this assumption of scalability of the calibration process pre-application testing of this methodology was executed. The Santa Barbara data set used for this research was resampled to ¼ of its full image resolution. A coarse calibration scenario (section 3.2.3.1) using the statistical control years {1967, 1976, 1986, 1998} was then executed on the full and ¼ resolution input. The calibration

results were then scored and sorted as described in sections 5.5.2 and 5.5.3 respectively. A summary of the scoring results is given in Table 3-1.

Full Resolution Results						**1/4 Resolution Results**					
		Range						**Range**			
Coeff	**Best**	start	stop	step	**Count**	**Coeff**	**Best**	start	stop	step	**Count**
disp	50	26	50	6	5	disp	50	40	60	5	5
breed	25	25	49	6	5	breed	1	0	12	3	5
spread	100	76	100	6	5	spread	50	40	60	5	5
slope	100	76	100	6	5	slope	75	65	85	5	5
road grav	50	0	50	10	6	road grav	1	0	50	10	6

Table 3-1: Coarse calibration results for full and 1/4 resolution input data

Results of this experiment showed that SLEUTH is not scalable across image resolutions. For all of the coefficients except dispersion the top scores different between the two calibrations. More importantly the *range* selected for the next phase of calibration using the ¼ data was not only different, but in some cases *excluded* the range selected from the full resolution calibration. Using resampled data as a methodological portion of brute force calibration will necessarily exclude the set of coefficients that would best apply to the full resolution data.

This difference is primarily due to the action of the spread_coefficient upon *edge growth*. *Edge growth* will propagate from an urban cluster no more than one neighborhood's distance in a single growth cycle. If the full resolution grid is 30 m, the ¼ resolution will be 120 m. That means that in a single growth cycle for the full resolution data, *edge growth* occurs at a rate of 30 m per growth cycle while the resampled simulation spreads at 120 m per growth cycle. Given a similar goal of urban extent from the initial conditions, the resampled data simulation is able to reach the goal in the same

time period as the full resolution simulation by applying a lower spread coefficient value.

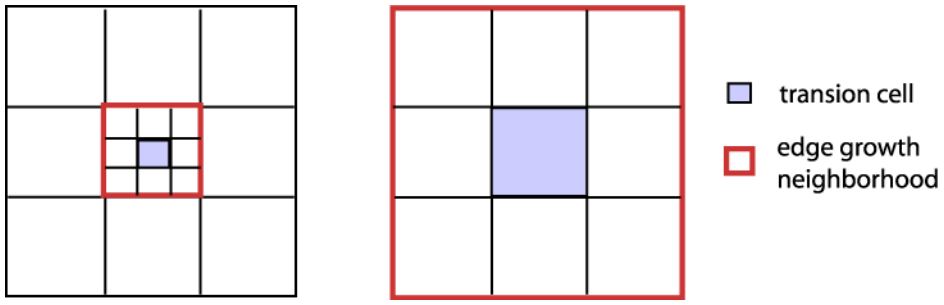

Figure 3-2: Difference in neighborhood extent between 1/4 and full resolution data.

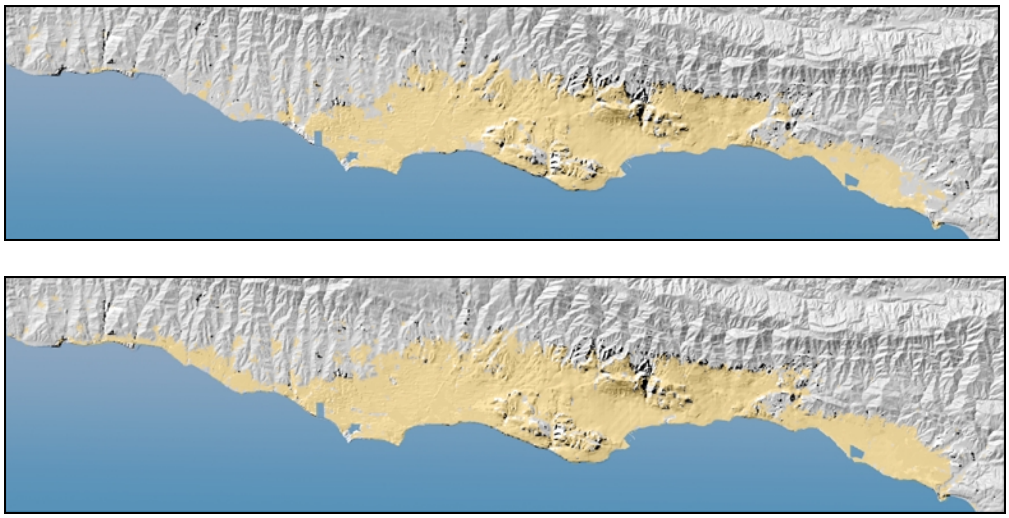

Figure 3-3: Simulated growth for full (top) and 1/4 (bottom) resolution data.

This difference in neighborhood spread-effect is easily illustrated in the data, as seen in Figure 3-3 where the yellow areas in the images represent modeled urban extent. These two simulations were initialized with the same parameters, except that one used 30 m data and the other used 120 m, and were run for 31 growth cycles (1967-1998). The ¼ resolution simulation shows much more growth to the East and West

of Santa Barbara (or the right and left of the image). Because the calibration process showed sensitivity to scaling the use of multiple image resolutions in the phases of coefficient search was abandoned. This application used full resolution data entirely to test SLEUTH temporal sensitivity to calibration controls.

3.2.4 Forecast Methodology

As stated above, SLEUTH forecasts rely on replicating growth trends from the past. Once a coefficient set is found that can best describe how urban change has occurred over time, these values are used to forecast future growth. The calibration process produces initializing coefficient values that best simulate historical growth for a region. However, due to SLEUTH's self-modification qualities, coefficient values that initialize the model for a date in the past may be altered by the simulation end date. Therefore, for *forecast* run initialization, the coefficient values at the simulation end date are used to initialize a new simulation into a future date. Using the best coefficients derived from calibration to run a large number of Monte Carlo simulations will produce a single set of averaged coefficients for the simulation end date. Using the BSS parameters derived from the simulation end date, a forecast run may be initialized.

For the image data, the most recent urban layer (the one that defined the calibration end date), the most recent transportation layer, and the exclusion and slope layers used in calibration, in addition to the background hillshade are used to initialize a forecast run. Growth rules are then applied to the data for a defined number of years. Forecasts are run in Monte Carlo fashion with 100 or more iterations. In addition to generating

annual urban growth probability maps, a log of coefficient and metric values may be written to a file as output.

Chapter 4

4 THE SOUTH COAST REGION

Figure 4-1: The South Coast study area detailed within California's Santa Barbara County.

The portion of Santa Barbara County used for this study, from here forward referred to as the *South Coast*, is located in coastal southern California about ninety miles northwest of Los Angeles (Figure 4-1). It extends from Rincon Point westward towards Gaviota and is bound by the Santa Ynez Mountains to the north and the Pacific Ocean to the south. It covers about 120 square km of Santa Barbara County. The nature of the area in which "the mountains meet the sea" has encouraged human development to occur laterally between steep slopes of the Santa Ynez and the coastal bluffs and beaches of the Pacific. The cities of the South Coast, Carpinteria, Santa Barbara, and Goleta, have grown up out of the more gently sloping areas in between the two along Highway 101, which runs centrally from east to west through the area. A large portion of the South Coast is part of the Los Padres National Forest and is protected from urban development. Because of the protected forest lands, the steep

slopes of the Santa Ynez, and the obvious building constraints of the ocean, the amount of land available to additional urbanization is quite limited.

4.1 Urban Centers

Santa Barbara is the county seat and center of the South Coast study region. The City had a population of about 89,600 in 2000. The economy is supported primarily by high tech industry, manufacturing, and tourism and retail business. Carpinteria is a small coastal community approximately 15 miles east of the City of Santa Barbara. The local population was over 14,000 in 2000. The predominant economic activity is greenhouses and other agriculture, high technology manufacturing, and tourism. Eight miles west of Santa Barbara, the newly incorporated city of Goleta has a population of approximately 87,000. The University of California at Santa Barbara and Santa Barbara Airport are primary employment sources in the area, followed by high technology, research and development, manufacturing, agriculture, and retail markets (SBCAG, 2001).

The South Coast experienced its first population boom in the decades following WWII. Brought on by the Baby Boom, average population growth rates from the 1950's through the 1960's, averaged 64%. The growth rate slowed dramatically in the 1970's to 13%, experienced an increase in the 1980's to 24% and fell again to 11% in the 1990's. The rate of urbanization of non-urban lands, on the other hand, experienced a more gradual decline. It's high occurred from the 1950's through the 1960's at 39%. In the 1970's it began to decline through the next decades to 36%, 22% in the 1980's and ending at 18% in the 1990's. The urbanization growth rate did not begin as high as the population growth rate, and decreased more slowly, indicating

a historic trend towards less dense residential housing stock as time goes on (SBCAG, 2001).

Santa Barbara County faces a demand for additional housing for between 104,000 and 247,000 people in the next 30 years (DOF, 2000). *Buildout* is the maximum planned capacity of an urban area based on its county designed current General Plan. At current growth rates, South Coast residential buildout accommodates less than 8 years of population growth. After that, if population growth rates remain stable, more land will need to be converted to residential uses unless housing density and/or household sizes increase significantly (SBCAG, 2001).

Several influential factors that will shape the growth rate of the South Coast over the next 30 years are already in place. The City of Santa Barbara historically has taken an anti-growth approach towards population expansion. This is especially evident in the affluent and low-density areas of Hope Ranch and Montecito. The North County of Santa Barbara on the other hand, with an abundance of open range and agricultural land, has always welcomed urban development. The newly incorporated city of Goleta will be hungry for the tax dollars a growing population can bring, but in this semi-arid and drought prone region, providing a secure water supply for an expanding populace is increasingly difficult. Finally, UC Santa Barbara, long the largest employer in the county, has reached its student capacity. Unless another type of industry or business experiences large and stable expansion, a primary source of employment opportunity in the area has stabilized.

Chapter 5

5 METHODS

5.1 Spatial-Temporal Data Base

In a geographic information system (GIS) database, input data for model calibration was compiled. GIS assisted in the generation, classification and formatting of the required data layers. Unless otherwise noted all GIS processing was completed using ESRI's Arc/Info. Data of varying types and dates were georeferenced to create a profile of urban development in the Santa Barbara region over space and time. The common geographic projection was Albers Equal Area. Specifics of classifying and formatting types are described below. After each data type was classified correctly, they were clipped to the same map extent and transformed to raster grids at 30 m resolution. Because the elevation data used was 30 m resolution, and the only inherently raster data source, this resolution was used for all data layers. The grid dimensions were 2074 columns by 486 rows. Representations of input data are included in Appendix A.

5.1.1 Urban

Aerial photographs of the Santa Barbara study area for the years 1929, 1943, 1954, 1967, 1976, 1986 and 1998 were scanned and georeferenced using ESRI's ArcView. Using on-screen digitization, the extent of built structures was digitized. This polygon data was then converted to raster at a resolution of 30 m, forming binary grids of urban/non-urban classes.

5.1.2 Transportation

The United States Census Bureau's TIGER 1999 line files of roads were downloaded from the TIGER website (http://www.census.gov/geo/www/tiger/) for the South Coast. These data were used as a starting point for assembling the weighted transportation layers. The classes highway, state route, and primary road were grouped together in the class Primary Road. Data of the Primary Road class were given a value of 100. The TIGER secondary road classification was also used and given a value of 50. Non-road data had a value of zero. This classification structure formed the 1998 roads layer.

Hardcopy transportation maps and aerial photography from the years 1929, 1943, 1954, 1967, 1976, and 1998 were used as ancillary data to create historical roads layers. Working back through time, the absence and classification of roads were noted and deleted from the layer if not present or demoted in value if its classification had changed. Dates selected for transportation input were intended to match urban layers as closely as data would allow.

5.1.3 Topography / Slope

The United States Geological Survey's 30 m digital elevation model (DEM) data were used as source data for the slope layer. The DEM was transformed to percent slope and then truncated to integer values (from floating point.) This truncation of values was performed so that the values found in the slope data would not exceed the 256 allowed by model input image format requirements.

5.1.4 Non-Urban / Excluded

The exclusion layer relied primarily on the Santa Barbara County Assessor's Office parcel map (1997) and Santa Barbara County government ownership map to identify

areas where urbanization would not occur. Los Padres National Forest, park lands, and privately held lands designated as preserves, as well as "waste" lands were selected for this category. In addition to the Pacific Ocean, the terrestrial water classes of rivers and reservoirs were excluded from urban growth. These classes were grouped together to form a binary excluded / non-excluded layer.

5.1.5 Background Hillshade

The hillshade layer is used as a background image for model image output and was derived from the same DEM used to generate the slope layer. Using the default settings for the Arc/Info command HILLSHADE, the DEM was transformed into a grayscale hillshade raster depicting South Coast topography.

5.2 Input Image Formatting

SLEUTH requires grayscale Graphic Image Files (GIF) as input. Because GIF is not an export option from Arc products, raster data were transformed first to TIF and then, using the xv image tool, were reformatted as GIFs. For all images, 0 is a null value, while $0 < n < 256$ is a "live", or existing, value.

Format standards for all data types:

- Grayscale GIF images
- Images are derived from grids in the same projection
- Images are derived from grids of the same map extent
- Images have identical dimensions (row x column count is consistent)
- Images follow the required naming format

5.3 Calibration Scenarios

Three calibration scenarios were defined using the database's seven urban layers and are illustrated in Figure 5-1. By varying the input data, the number of control points for statistical comparison (or density) was altered. Also, in doing this, the number of

years being simulated (or duration) was changed to look at the efficacy of short-term and long-term historical databases.

5.3.1 Scenario 1(All__data)

The first scenario (All_data) used all seven of the urban inputs {1929, 1943, 1954, 1967, 1976, 1986, 1998} as control years for calibration and executed a long-term, "high density" control year calibration. This scenario calibrated the model for a duration of 69 years, from 1929 to 1998. The number of years between data layers ranged from 14 years to 9 years with an average of 11.5 years.

5.3.2 Scenario 2 (Recent_data)

The second scenario (Recent_data) executed the briefest calibration duration of 31 years by utilizing only the four most recent control years {1967, 1976, 1986, 1998}. This series of input also dropped the average duration between control years to 10.3 years. This scenario represents a short-term calibration utilizing data acquired from the mid-sixties to present.

5.3.3 Scenario 3 (Sparse_data)

The third scenario (Sparse_data) had the same duration as the first (from 1929 to 1998) but only four control years were used {1929, 1954, 1976, 1998}. By selecting only every other control year from the entire set the requisite four control points was achieved but the average duration between control years increased from 11.5 years to 23 years.

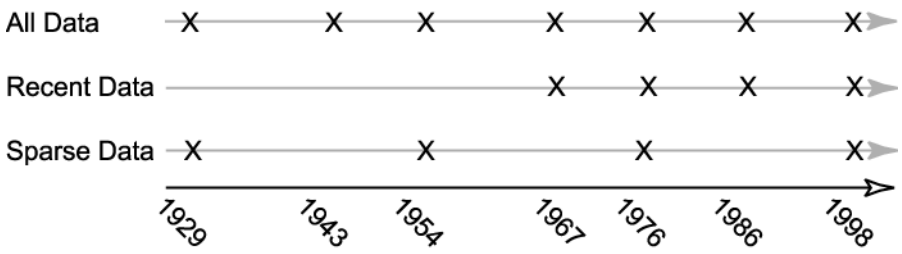

Figure 5-1: Calibration scenario temporal input composition

5.4 Self-Modification

The values used in the process of self-modification inherited from previous calibrations of the model (Clarke et al., 1997) were held as constants. These constants, used to determine if the system is experiencing accelerated or decelerated growth, as well as the values applied in self-modification, are defined in the scenario file. The values used for this application are listed in Appendix B.

5.5 Calibration

The brute force calibration process of previous SLEUTH applications is described in detail in section 3.2.

5.5.1 Pseudo-Parallel Processing

SLEUTH 3.0 version is written to run in a parallel computing environment. However, such an environment was not available for this research. Due to the large amount of computing power required to run the multiple calibrations required for this applications, a pseudo-parallel processing environment was created.

Since each run for a unique coefficient set is initialized with the same random number seed, an entire calibration scenario could be parsed into jobs and delegated to separate machines. Fourteen Silicon Graphics O_2 workstations were available, on a shared basis, for this work. For each phase of calibration, the three scenarios were divided

into multiple jobs, and these jobs were dedicated to workstations, one job per workstation. When the jobs were finished, the statistic files were concatenated by scenario and sorted.

5.5.2 Simulation Score Sorting

SLEUTH generates best-fit statistics for eleven metrics. These metrics are:

compare: compares the amount of modeled urban area to known urban area for the stop date year where $P_{modeled}$ is the modeled urban area and actual area for final year is (P_{actual}):

```
if (P_modeled < P_actual) {
   compare = (P_modeled / P_actual)
}else{
   compare = 1 - (P_modeled / P_actual)
}
```

pop: least squares regression score for modeled urban area compared to actual urban area for the control years

edges: least squares regression score for the modeled amount of urban perimeter , or edge, compared to actual urban perimeter for the control years

clusters: least squares regression score for modeled number of urban clusters compared to known number of urban clusters for the control years

cluster_size: least squares regression score for modeled average urban cluster size compared to known average urban cluster size for the control years

leesalee: a shape index, a measurement of spatial fit between the model's growth and the known urban extent for the control years 1 being a perfect match and 0 representing a spatial disconnect:

$s = (A \cap B)/(A \cup B)$

where A is modeled and B is actual urban area.

slope: least squares regression of average slope for modeled urbanized cells compared to average slope of known urban cells for the control years

%urban: least squares regression of percent of available pixels urbanized compared to the urbanized pixels for the control years

xmean: least squares regression of average longitude (calculated using column values) for modeled urbanized locations compared to average longitude of known urban locations for the control years

ymean: least squares regression of average latitude (calculated using row values) compared to average latitude of known urban locations for the control years

rad: $\sqrt{\left(std_x^{\,2} + std_y^{\,2}\right)}$ is a measure of urban dispersal

These metrics are generated for each control year. The simulated data is then compared to the metrics of the historical data and linear regression values are calculated. These best-fit values are written to the `control_stats.log` output file. The `control_stats.log` file is the primary file used to score the many runs executed during calibration.

The greater the number of metrics used for calibration, the more difficult it is to isolate and describe the factors that influence a successful calibration score. One of the objectives of this research is to describe calibration metric values and model coefficients, and explain how they affect model behavior. For this reason, a subset of five metrics was selected in order to decrease the number of influencing values that affect calibration. The four calibration metrics used in Clarke et al. (1997) (population, number of edges, number of clusters and Lee Sallee) were applied here with one addition: average cluster size. For Santa Barbara, these five metrics best captured the physical dynamics of urban expansion over the data period. The metric regression scores were weighted evenly and multiplied. Their products supplied a score of simulation performance for each coefficient set, and were sorted in descending order.

5.5.3 Coefficient Range Selection rules

A series of rules formed a guideline for selecting top calibration scores and narrowing the range of best performing coefficients. These rules were followed hierarchically:

1. Decrease coefficient range from previous phase (e.g.; from {0 - 100} to {0 - 25})

2. Decrease step increment from previous phase (e.g.; from increment = 25 to increment = 5)

3. Keep range increments between four and six, five being the goal, while being "true" to range (e.g.; {0 - 25 x 5} has six increments. Alternatively, {0 - 24 x 6} has five increments and is preferable. The trade-off here is CPU vs. solution space resolution. If the previous phase of calibration has narrowed the range (e.g.; to {0 - 25}) decreasing the number of increments while still covering almost all of the range is optimal.

4. Focus on top three sorted scores

5. If step increment does not exactly hit all top scores in range, give precedence to best score (i.e.; If, from a coefficient set of {0, 25, 50, 75, 100}, 0 and 25 defined the range for a coefficient's top three sorted scores, but 25 did better than 0, then an appropriate range and increment selection for the next phase would be: {1 - 25 x 6} rather than {0 - 24 x 6}.)

6. If a single coefficient value shows very strongly, search around that value (e.g.; for a coefficient, all top scores = 25. In the next phase, range and increment would be {15 - 35 x 5})

5.5.4 Multiple Scenario Calibration

The three calibration scenarios All_data, Recent_data, and Sparse_data were executed in pseudo-parallel on SGI O_2 workstations. Concatenated `control_stats.log` files were brought into Microsoft Excel as spreadsheets. Macros were used to multiply the selected calibration metrics: population, edges, clusters, cluster size, and Lee Sallee, and sort the resultant scores. Using the coefficient range selection rules, top performing coefficient sets were identified and the solution space of each coefficient was decreased before commencing the next phase of calibration.

Through the three phases of brute force calibration (coarse, fine, and final) a single set of coefficients for each calibration scenario were identified as best simulating the historical urban layers used in their respective scenario. By setting the *WRITE_AVG_FILE* flag to "*YES*" in the SLEUTH execution (`scenario`) file, these runs wrote to output file `avg.log` averaged metrics and coefficient values for each control year. These `avg.log` files were brought into Excel for analysis. An average of each scenario's ending coefficient values, or best solution set (BSS) were used to initialize a forecast.

5.6 Multiple calibration Scenario Forecasting

The three calibration scenarios each produced a BSS. Each set was used to initialize a run of simulated growth in SLEUTH from 1998 to 2030. 100 Monte Carlo simulations were used in each run. The `avg.log` files were used for analysis. Classified annual urban probability images were brought into ArcInfo Grid for spatial analysis. These maps were also brought into Adobe Photoshop for image processing as final products.

Chapter 6

6 RESULTS AND SUMMARY

6.1 Calibration

6.1.1 Metric Behavior

In order to measure the success of modeled growth, a simulation must be compared to historical urban data. The averaged metric types used for calibration (population, edges, clusters, cluster size, and Lee Sallee) were noted in the derive runs of the three calibrating scenarios. These values are recorded in Appendix C. In the metric graph series (Figures 6-1 through 6-4) these values are plotted against the control year data, or *base statistics*. The Lee Sallee (Figure 6-5) is not plotted against the base statistics since the control compared to itself would always have a perfect r^2 of 1.0. The Sparse_data scenario only had the years 1929, 1954, 1976 and 1998 as statistical controls during calibration. However, during the derive run, r^2s of the years in between (1943, 1967, 1986) can be produced and are included in these graphs to give additional information on the dynamics of that scenario's simulation.

6.1.1.1 All_data Scenario

The population metric (Figure 6-1) slightly overestimated growth in the first control years 1943 and 1957 and underestimated in the later years of the simulation. All_data did little to capture the variation in the number of urban edges and consistently underestimated their value (Figure 6-2). The number of urban clusters was most closely simulated in this scenario, with only small underestimation in the years {1956, 1967, 1976} and a larger underestimate in the final year when the base statistics

experienced a sharp increase (Figure). Similarly, the average number of pixels within each urban cluster was modeled closely until the final control years where the base statistics increased and then decreased sharply (Figure 6-4). The simulation followed a middle ground between these two by under and overestimating 1986 and 1998 respectively. The Lee Sallee (Figure 6-5) shape metric was at its best (0.6) when measured at the first control year. After that it decreased, leveled off, and then increased moderately in the final years to finish at 0.51 for an overall r^2 of 0.47.

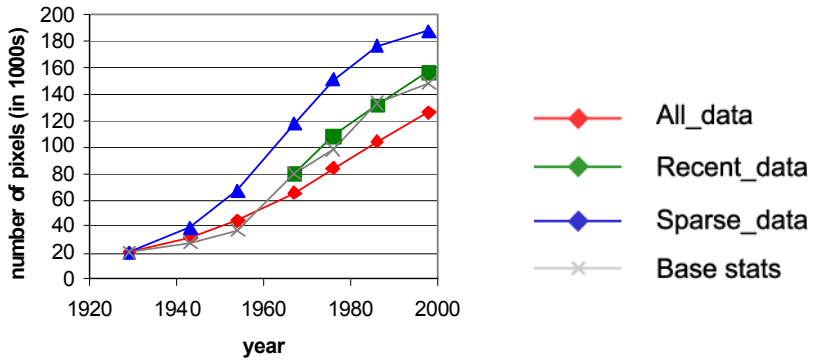

Figure 6-1: Urban area metric (pop) for calibration

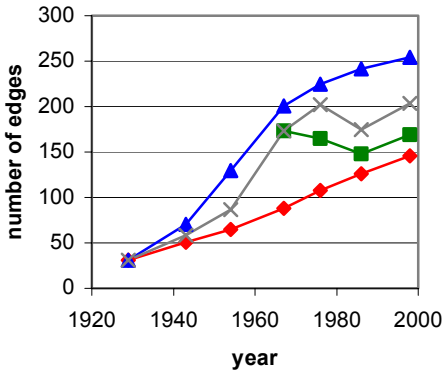

Figure 6-2: Urban metric (`edges`) for calibration

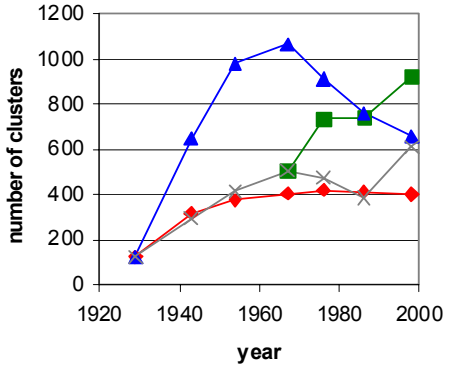

Figure 6-3: Number of urban clusters metric (`clust`) for calibration

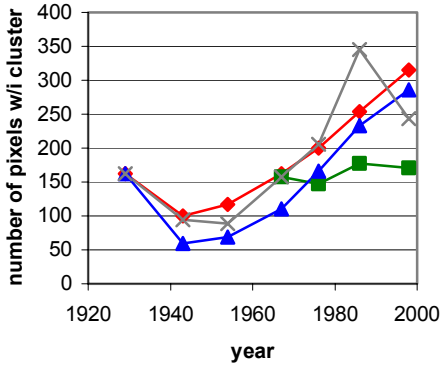

Figure 6-4: Average urban cluster size metric (`clust_size`) for calibration

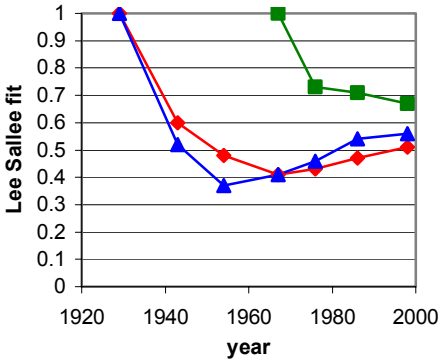

Figure 6-5: Lee Sallee shape metric (`leesal`) for calibration

6.1.1.2 Recent_data Scenario

Following the almost linear growth in the final thirty years of the simulation, Recent_data slightly overestimated population for 1976 and 1998, and fit 1986 almost exactly (pop r^2=0.94) (Figure 6-1). Number of edges is underestimated, but the steep decrease and increase of values in the final years is modeled fairly well (Figure 6-2). Recent_data begins with an overestimate of number of clusters that seems inversely

related to the control data for 1976 and 1986. The final year, 1998, is also overestimated, but the rate at which the value increases closely follows the control data trend (Figure 6-3). Average cluster size is underestimated and the model is unable to capture the 1986 peak in the control data (Figure 6-4). Recent_data generated the best Lee Sallee scores with a low in the final year of only 0.67 (Figure 6-5). However, unlike the scenarios that ran for a longer duration, an improvement in the score over time was not seen.

6.1.1.3 Sparse_data Scenario

While the third calibration generated a nice "S-curve" for the population metric (Figure 6-1) it consistently overestimates the number of urban pixels. Number of edges is moderately overestimated for this scenario (Figure 6-2), but the largest deviation from the control data comes in 1986 where the model misses the dip in the control data trend. Number of clusters (Figure 6-3) is largely overestimated for the duration of the simulation, but the final control year is almost an exact match. Average cluster size (Figure 6-4) follows a similar trend as All_data, but the control data is consistently underestimated until 1986 when the control data takes a sharp decline and is consequently overestimated. The Lee Sallee reached a low of about 0.3 in 1957 and then consistently improved for the remainder of the simulation to finish at 0.5 (Figure 6-5).

6.1.2 Metric Regression Scores

The products of the five calibration metrics best-fit scores were used to sort and identify the best performing coefficient sets and are recorded in Appendix C. The top product values across the three phases of calibration are shown in Figure 6-6. The

regression scores of each calibration metric that made up the top product score are illustrated in Figure 6-7 through Figure 6-11. The phases of calibration, *coarse*, *fine* and *final* are indicated on the graphs as *1*, *2* and *3*, respectively.

6.1.2.1 All_data Scenario

Of the three scenarios, All_data generated the least successful simulations when considering the product of the five calibration metrics used for sorting (Figure 6-6). It was able to improve consistently through the calibration phases, but scores remained lower than the other two scenarios. All_data population scores (Figure 6-7) were high and remained around 0.98 through the three phases of calibration. The number of edges (Figure 6-8) and average cluster size (Figure 6-10) both decreased in performance in the fine phase and then leveled off for the final phase. Lee Sallee (Figure 6-11) on the other hand, increased from 0.39 to 0.47 from the coarse to fine

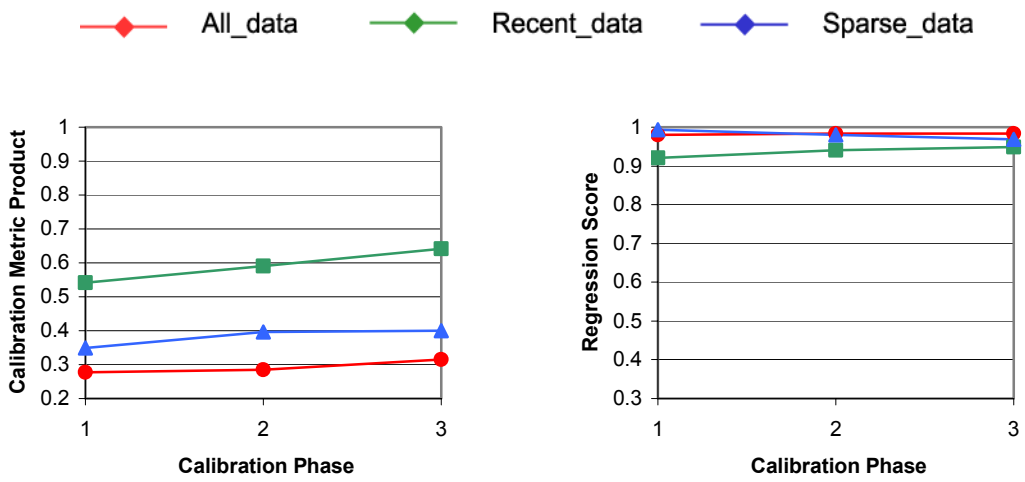

Figure 6-6: Calibration metric product score

Figure 6-7: Urban area (pop) regression scores

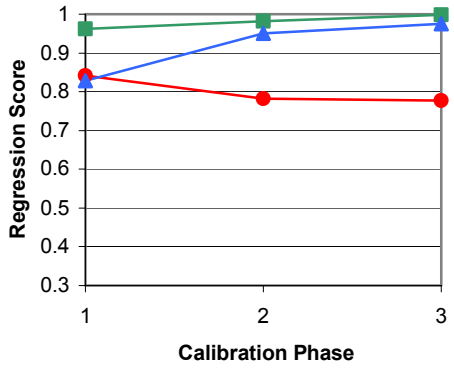

Figure 6-8: Urban (`edges`) regression scores

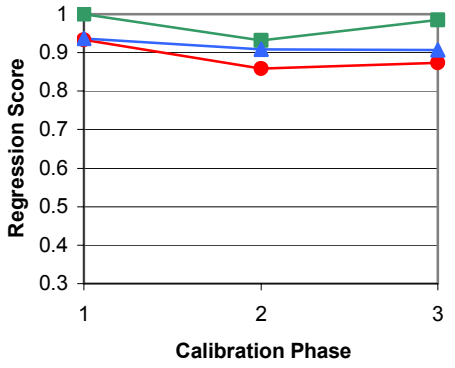

Figure 6-9: Number of urban clusters (`clust`) regression scores

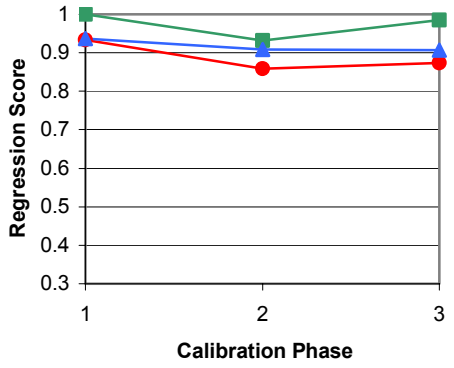

Figure 6-10: Average size of urban clusters (`clust_size`) regression scores

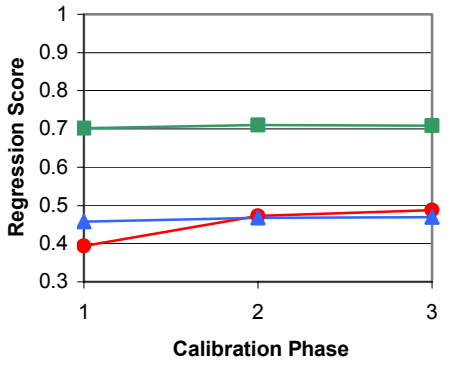

Figure 6-11: Lee Sallee (`leesal`) regression score

phase before leveling off from fine to final. This was the largest improvement of any scenario for the Lee Sallee. The average number of clusters (Figure 6-9) remained stable through fine calibration and then increased in the final phase.

6.1.2.2 Recent_data Scenario

Recent_data calibration product scores (Figure 6-6) improved steadily through the three phases of calibration from 0.54 to 0.64. For the population regression scores

(Figure 6-7), Recent_data performed least well of the three scenarios beginning at 0.92 from the coarse phase and finishing at 0.95. The number of urban edges regression also improves through the phases of calibration increasing from 0.96 in the coarse phase to 0.99 in the final (Figure 6-8). The average number of clusters improved from 0.87 to 0.96 in the fine phase and then increased only slightly to 0.97 in the final phase (Figure 6-9). Average cluster size was just under a score of 1.0 after the coarse phase and then dropped to 0.93 before improving to 0.98 in the final phase. Recent_data had little variation in the Lee Sallee score maintaining a score around 0.71 for the three phases.

6.1.2.3 Sparse_data Scenario

Unlike the other two calibrations, after improving from the coarse to fine phase of calibration, the Sparse_data product score leveled off from the fine to final phase topping out at 0.4 (Figure 6-6). The population regression score got consistently worse from a high of 0.99 to 0.97 in the final phase (Figure 6-7). The number of urban edges improved greatly between a coarse phase value of 0.83 to fine at 0.95 and finished at 0.97 (Figure 6-8). The average number of clusters increased slightly after the coarse phase to level off at 0.99 (Figure 6-9). The average cluster size decreased after the fine phase from 0.94 to 0.91 (Figure 6-10). The Lee Sallee improved little through the phases of calibration and remained close to 0.46 (Figure 6-11).

6.1.3 Coefficient Solution Space

Each of SLEUTH's five coefficients may range between {0 – 100}. The process of selecting a set of coefficients for each of the three calibrations created a unique solution space for each parameter (Figure 6-12 - Figure 6-16). These values are listed

in Appendix A. Because each coefficient began with a range of {0 – 100} in the coarse phase of calibration, this range is assumed and not represented in the diagrams. Instead, the first values on the graph indicate the range used to initialize the fine phase of calibration after selecting the top scores from the coarse run.

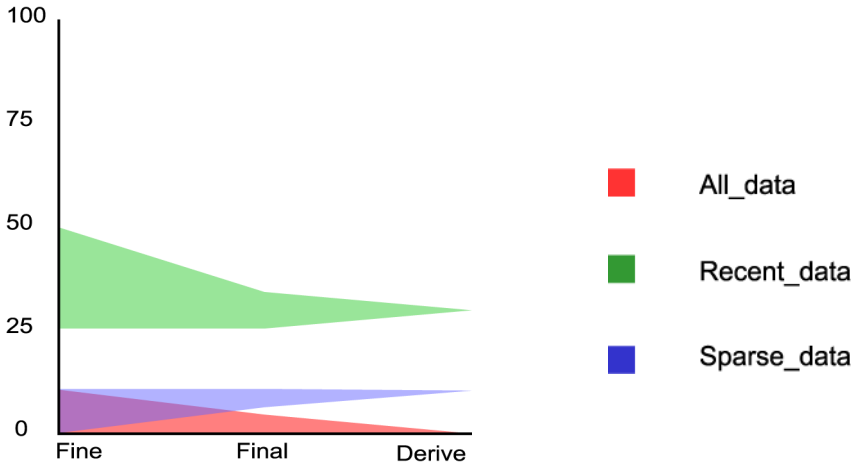

Figure 6-12: Dispersion calibration space

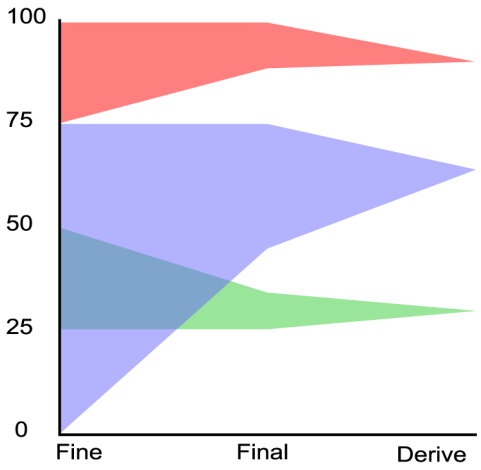

Figure 6-13: Breed calibration space

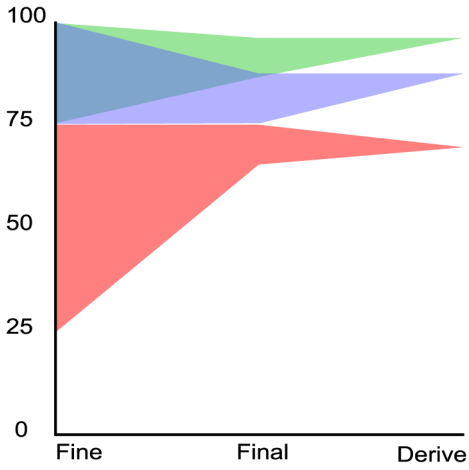

Figure 6-14: Spread calibration space

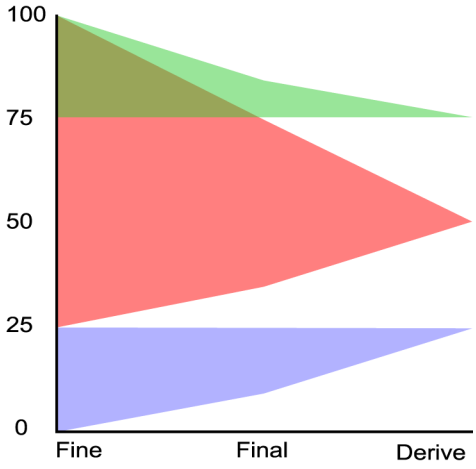

Figure 6-15: Slope resistance coefficient space

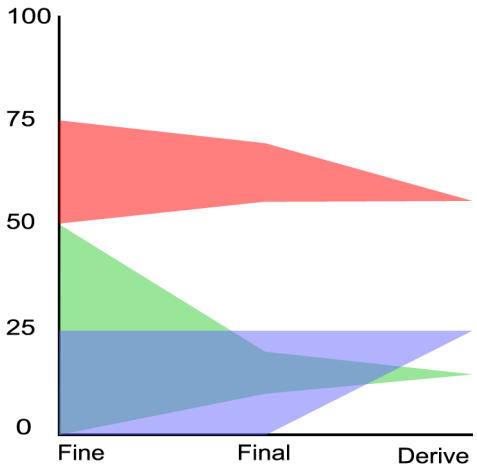

Figure 6-16: Road gravity space

6.1.3.1 All_data Scenario

The dispersion coefficient solution space for All_data narrowed easily (Figure 6-12). The coarse phase revealed a tendency for the coefficient to be low, so a range of {1-12, 4} (start-stop, step) initialized the fine run and {1-5, 1} set up the final run. A dispersion value of 1 performed the best throughout all phases of calibration. Coarse results for breed (Figure 6-13) showed that the breed coefficient wanted to remain at the high end of the range. A range of {75-99, 5} initialized the fine phase and this was adjusted upwards again for final calibration {87-99, 3} with a best final value of 90, which was used to initialize the derive run. The spread coefficient range (Figure 6-14) was narrowed to the middle portion of its range through coarse calibration: {25-75, 10}. A best value of 69 was derived from the final calibration phase range of {66-75, 3}. For All_data slope resistance proved to be the most difficult coefficient to select a best value for Figure (6-15). After coarse calibration its range was still large ({25-100,

15}) and that was only narrowed by the fine phase to {35-75, 8} from which a best score of 51 was derived. Road gravity (Figure 6-16) had a range of {51-75, 6} after coarse calibration and {57-69, 3} after fine. From final calibration a best score of 57 was selected.

6.1.3.2 Recent_data Scenario

A range of {26-50, 6} was selected for the dispersion coefficient after the coarse phase of calibration (Figure 6-12). This range was further narrowed to {26-34, 2} for the final phase which selected a best value of 30. For the fine calibration phase, the breed coefficient had a range of {25-49, 6} which was reduced to {25-33, 2} (Figure 6-13). From the final phase, 31 was selected as the best coefficient value. The spread and slope resistance coefficient both produced best performance ranges of {76-100, 6} after the coarse phase (Figure 6-14). 96 was selected as the best performing value for the spread coefficient after narrowing the range to {88-96, 2} for the final phase. From a final range of {76-84, 2} for the slope resistance coefficient a value of 76 was selected (Figure 6-15). The road gravity range (Figure 6-16) could only be reduced by half after the coarse phase to {0-15, 10}, but this was narrowed to {10-20, 2} by the final phase which generated a best performing coefficient value of 14.

6.1.3.3 Sparse_data Scenario

The dispersion coefficient easily narrowed to a best value of 11 from a range of {0-12, 4} in the fine phase and {8-12, 1} in the final phase (Figure 6-12). The breed coefficient range was more difficult to reduce (Figure 6-13). After the coarse phase only a small part of the range was excluded leaving the values {0-75, 15} to be

examined. This led to a final phase initial range of {45-75, 6} which generated a best breed coefficient value of 63. The spread coefficient remained at the high end of the range producing a best value of 88 for the derive run (Figure 6-14). The slope resistance coefficient was narrowed to the first quarter of the range for the fine run {1-25, 6} and then remained at the top of that range with 25 being selected as the initial value for the derive run (Figure 6-15). After narrowing the road gravity coefficient to {1-25, 6} after the coarse phase of calibration, the range could not be further narrowed for final calibration (Figure 6-16). Consequently, the step increment was decreased in order to explore the range at a finer scale: {0-25, 5}. The final phase generated a best road gravity coefficient value of 25.

6.1.4 Coefficient Behavior

The self-modification qualities of SLEUTH make it probable that coefficient values will not remain static throughout a simulation. Averaged coefficient values taken from the derive runs (Figure 6-17 - Figure 6-21) illustrate the dynamic behavior of the parameters during model execution.

6.1.4.1 All_data Scenario

All_data maintained a low dispersion coefficient value for the duration of the simulation beginning at 1 and finishing at 2 (Figure 6-17). The breed coefficient (Figure 6-18) increased from 90 to a maximum value of 100 by the first control year in 1943 where it remained for the duration of the simulation. The spread coefficient (Figure 6-19) also steadily increased from 66 to reach 100 by 1967 where it remained.

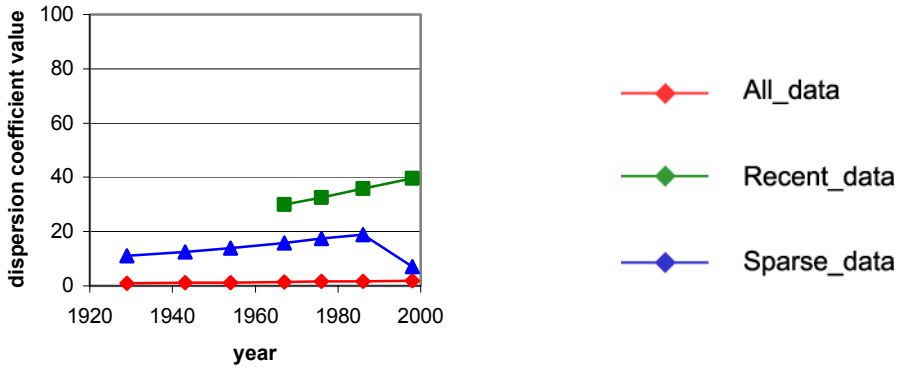

Figure 6-17: Dispersion coefficient values for calibration

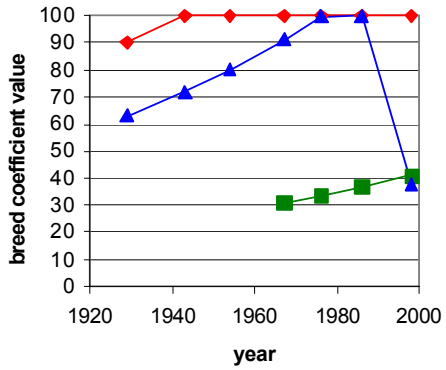

Figure 6-18: Breed coefficient values for calibration

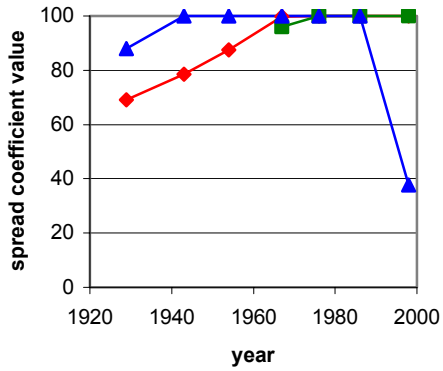

Figure 6-19: Spread coefficient values for calibration

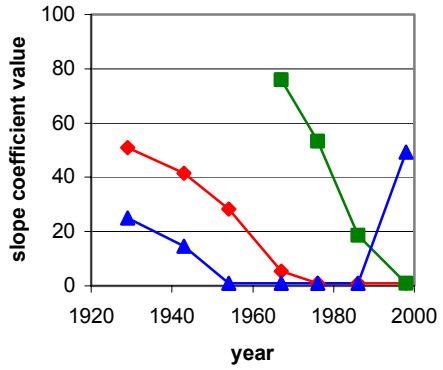

Figure 6-20: Slope resistance coefficient values for calibration

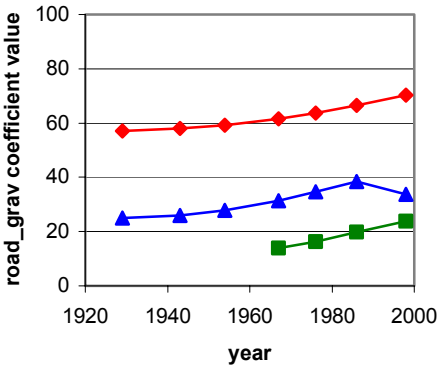

Figure 6-21: Road gravity coefficient values for calibration

Figure 6-20 shows how, as the other coefficients increased, slope resistance decreased from 51 to reach a minimum value of 1 by 1976. Note how the rate of decrease lessens for the period of 1967 to 1976. This change corresponds to the leveling off of the spread coefficient value. The road gravity coefficient increases steadily throughout the simulation to go from a value of 57 at initialization to 70 at the simulation stop date (Figure 6-21).

6.1.4.2 Recent_data Scenario

The dispersion coefficient (Figure 6-17) steadily increased at a moderate rate from 30 in 1967 to 40 in 1998. The breed coefficient (Figure 6-18) followed a similar trend and increased from an initial value of 31 to 41 in the final simulation year. Beginning at 96, the spread coefficient (Figure 6-19) quickly reached its maximum value of 100, where it remained. The slope coefficient (Figure 6-20) decreased steadily to reach its minimum value of 1 by the final control year. Road gravity was initialized at 14 and then increased to a value of 24 by 1998 (Figure 6-21).

6.1.4.3 Sparse_data Scenario

Sparse_data, unlike the other two calibration scenarios, went from a BOOM to a BUST state in the historical, or calibration phase of simulation. The others did not experience this state change until the forecasting phase. The dispersion coefficient (Figure 6-17) increased at a moderate rate through 1986 and then dropped off quickly by 1998. The breed coefficient (Figure 6-18) increases to the year 1976 when it reached 100 and leveled off at this maximum until dropping sharply to a value of 38 in 1998. The spread coefficient (Figure 6-19) reached its maximum by the second control year where it remained until dropping to 38 in the final control year. Similarly, the slope resistance (Figure 6-20) reached its minimum by 1957 and remained there until the shift to the BUST state after 1986, and rising to 49 by 1998. Road gravity (Figure 6-21) increased from an initial value of 25 in 1929 to a high of 39 in 1986 before descending to 34 in 1998.

6.2 Forecasting

6.2.1 Metric Behavior

In order to observe the dynamic behavior of forecasted urban growth, a simulation must be compared to historical urban data. The averaged metric types used for calibration (population, edges, clusters, and cluster size) were tracked in the forecast runs of the three calibration scenarios. In the metric graph series (Figure 6-22 through Figure 6-26) these values are plotted every five years until the temination date 2030. The Lee Sallee and metric regression scores could not be measured because there is no control data for the future that the simulation could be compared to.

6.2.1.1 All_data Scenario

The number of urban pixels increased steadily in the first portion of the simulation before leveling off at ~ 200,000 pixels in 2020 (Figure 6-22). After an initial brief increase, the number of urban edges gradually decreased to 19,607 in 2030 (Figure 6-23). Initialized at 611 in 1998, the number of urban clusters (Figure 6-24) experienced a radical increase to 944 by the year 2000. Here it peaked out and decreased just as dramatically until it reached 585 in 2010, at which point the rate of decrease began to slow for the duration of the simulation. Average urban cluster size on the other hand (Figure 6-25) decreased sharply in the first years of the simulation and then increased quickly from 166 in the year 2000 to 392 in 2015 when the rate of increase began to slow to end at 445 in 2030.

6.2.1.2 Recent_data Scenario

The Recent_data forecasted number of urban pixels (Figure 6-22) increased quickly from ~148,500 in the first half of the simulation and gradually began to level off through the end of the simulation to generate an averaged value of ~210,000 for the year 2030. After a small dip, the number of urban edges (Figure 6-23) increased moderately from its initial value of 20,300 to finish at 22,143. In a similar trend as with All_data, the average number of clusters (Figure 6-24) experienced a radical increase from the initial value of 611 to 988 in the first few years of the forecast. This value began to decrease after 2005 at a moderate rate to reach 791 by the stop date. The average cluster size (Figure 6-25) increased at a steady rate rising from 243 in 1998 to 265 in 2030.

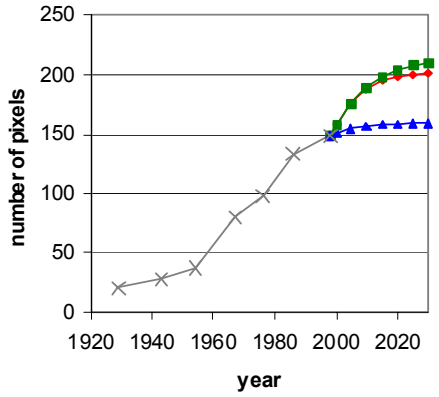

Figure 6-22: Urban area metric (`pop`) for forecasting

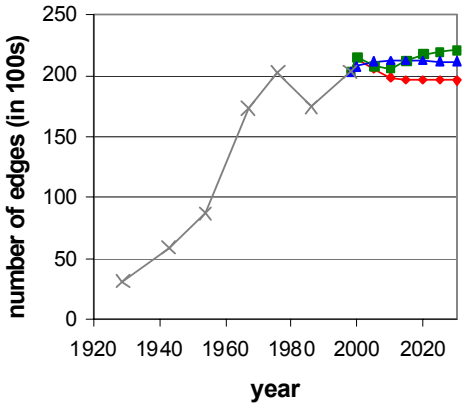

Figure 6-23: Urban metric (`edges`) for forecasting

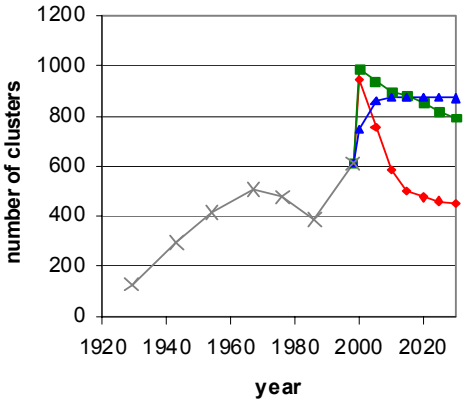

Figure 6-24: Number of urban clusters metric (`clust`) for forecasting

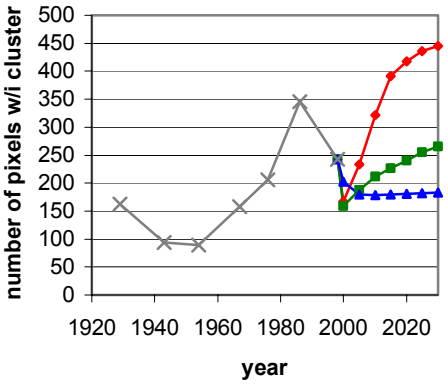

Figure 6-25: Average size of urban clusters metric (`clust_size`) for forecasting

6.2.1.3 Sparse_data Scenario

The number of urban pixels (Figure 6-22) increases by less than 1000 pixels in the over thirty simulated years of the forecast, from 148,548 to 159,167. The number of

edges (Figure 6-23) increased from 203 to 212. The average number of clusters (Figure 6-24) increased less radically than the other two calibrations and plateaued at about 875 in 2015. The average cluster size (Figure 6-25) decreased from 243 to 179 by 2010 where it remained for the duration of the simulation.

6.2.2 Coefficient Behavior

6.2.2.1 All-data Scenario

The dispersion coefficient maintained a value of about 1 for the duration of the forecast simulations (Figure 6-26). The breed and spread coefficients remained at 100 until 2010 and then decreased rapidly to a value of 15 by 2030 (Figure 6-27 and Figure 6-28respectively). Slope resistance had a value of 1 until 2010 at which time it began to increase to reach a value of 100 by 2030 (Figure 6-29). Road gravity increased moderately through 2010 and then in 2015 began to steadily decrease (Figure 6-30).

6.2.2.2 Recent_data Scenario

As during the derive run over the historical data, the dispersion and breed coefficients followed very similar trends during the forecast (Figure 6-26 and Figure 6-27 respectively). They began with a value of ~40, increased moderately to a high of ~44 through the simulation date 2010, and then began a slow descent to ~38 in the stop year 2030. Spread maintained its maximum value of 100 until 2015 when it began to moderately decrease to reach a value of 85 at the end of the simulation (Figure 6-28). The slope resistance coefficient (Figure 6-29) remained at 1 until the simulation date 2015 at which time it began to rapidly increase to arrive at 93 by the stop date. Road gravity (Figure 6-30) showed moderate change attaining a high of 28 in 2010 before moderately descending to a value of 19 in 2030.

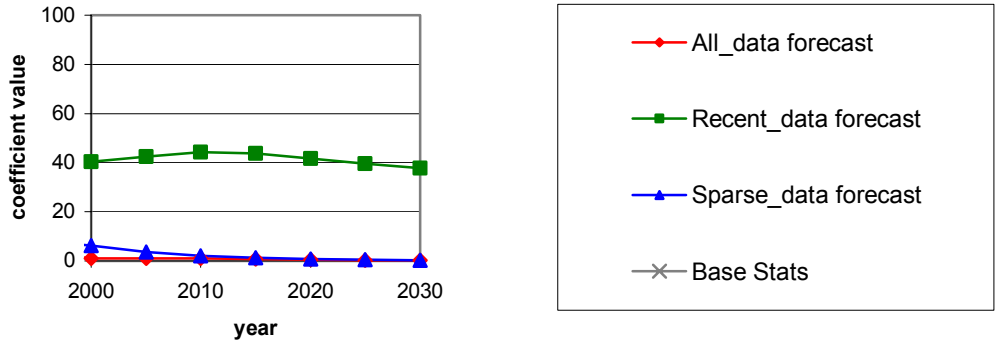

Figure 6-26: Dispersion coefficient values for forecasting

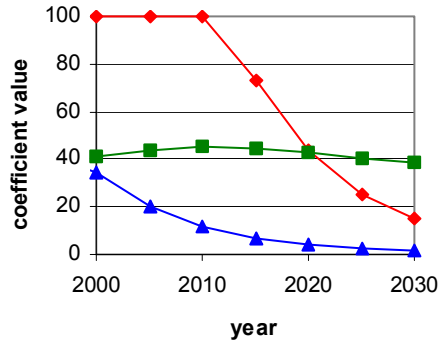

Figure 6-27: Breed coefficient values for forecasting

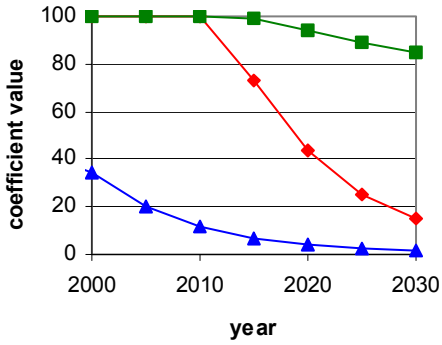

Figure 6-28: Spread coefficient values for forecasting

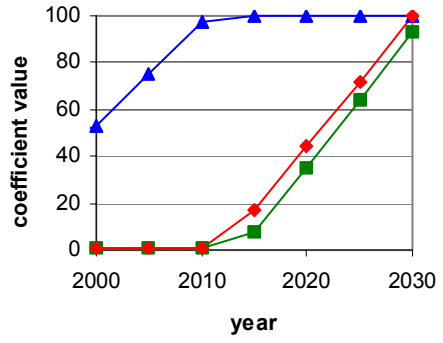

Figure 6-29: Slope resistance coefficient values for forecasting

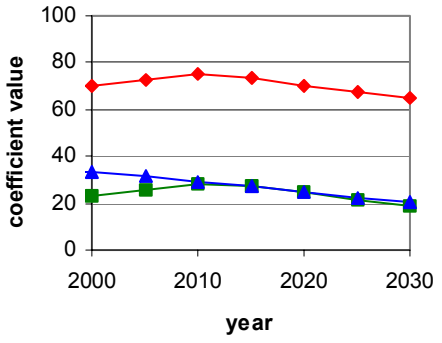

Figure 6-30: Road gravity coefficient values for forecasting

6.2.2.3 Sparse_data Scenario

The dispersion coefficient (Figure 6-26) decreased from 7 to a value of 1 by 2015 where it remained for the duration of the simulation. Breed and spread (Figure 6-27 and Figure 6-28respectively) decreased from an initial value of 37 to the minimum of 1 by the stop date of 2030. The slope resistance coefficient (Figure 6-29) was initialized at 49 and reached its maximum of 100 by 2015. The road gravity coefficient steadily decreased from 34 to 20 in the final year (Figure 6-30).

6.2.3 Multiple Scenario Forecast Maps

The probability forecast maps were brought into ArcInfo for simple image analysis. The images were classified by probability. The pixel counts of each of these probabilities are listed in Table 6-1.

	All_data	**Recent_data**	**Sparse_data**
100-95% probability	44127	49799	178
90-95% probability	2160	1715	705
80-90% probability	2294	1930	2376
70-80% probability	1548	1415	2288
60-70% probability	1227	1431	1986
50-60% probability	1032	1726	2101

Table 6-1: Pixel counts for 2030 urban forecast (excluding 1998 urban extent).

Forecast maps of simulated growth for the year 2030 were generated from the three forecast scenarios All_data, Recent_data and Sparse_data. These forecast runs were initialized with the calibrated BSS for each scenario and run for 100 Monte Carlo iterations. Two drawn boxes on the primary maps (Figure 6-31 – Figure 6-33) reference the detail figures located above the primary map.

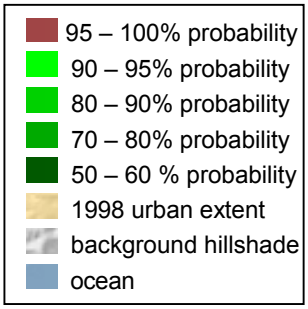

Figure 6-31b: detail of All_data 2030 forecast of the Gaviota area

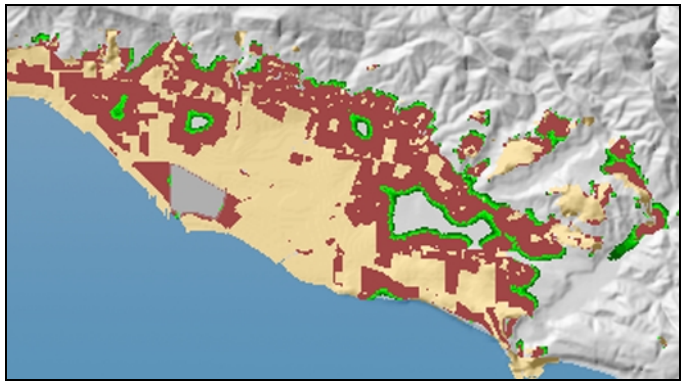

Figure 6-31a: detail of All_data 2030 forecast of the Carpinteria area

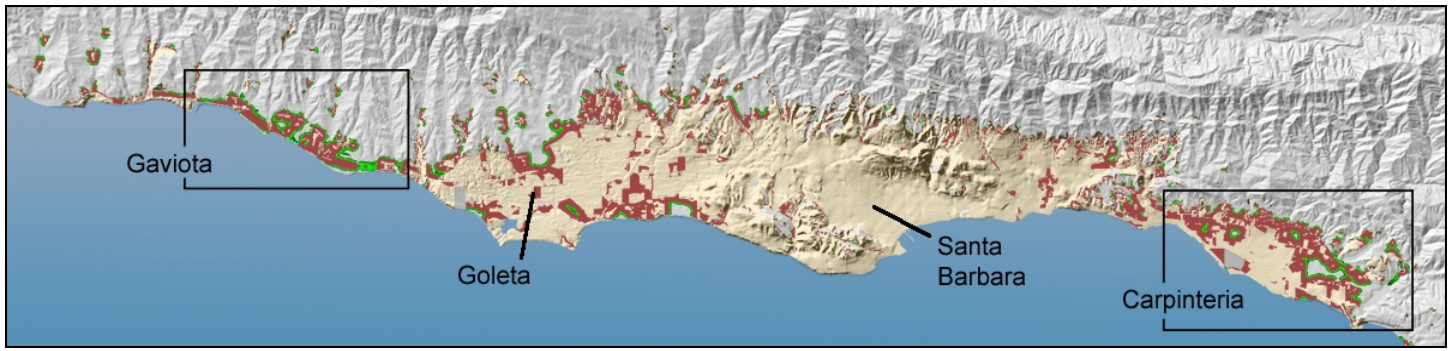

Figure 6-31: All_data urban probability forecast for the year 2030

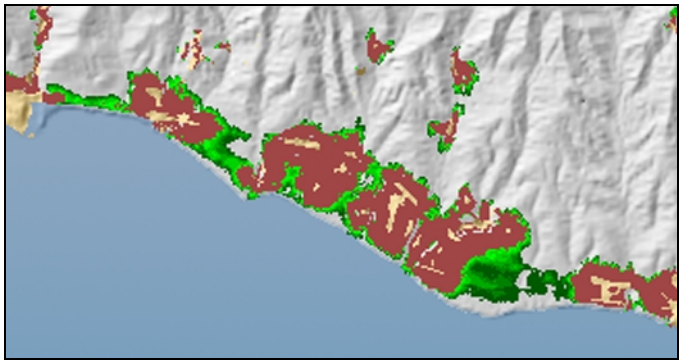

Figure 6-32b: detail of All_data 2030 forecast of the Gaviota area

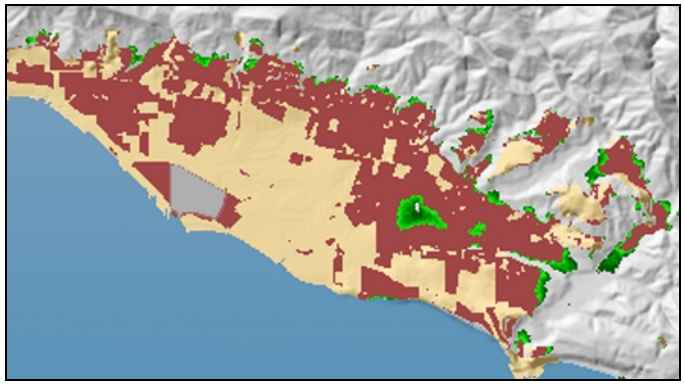

Figure 6-32a: detail of All_data 2030 forecast of the Carpinteria area

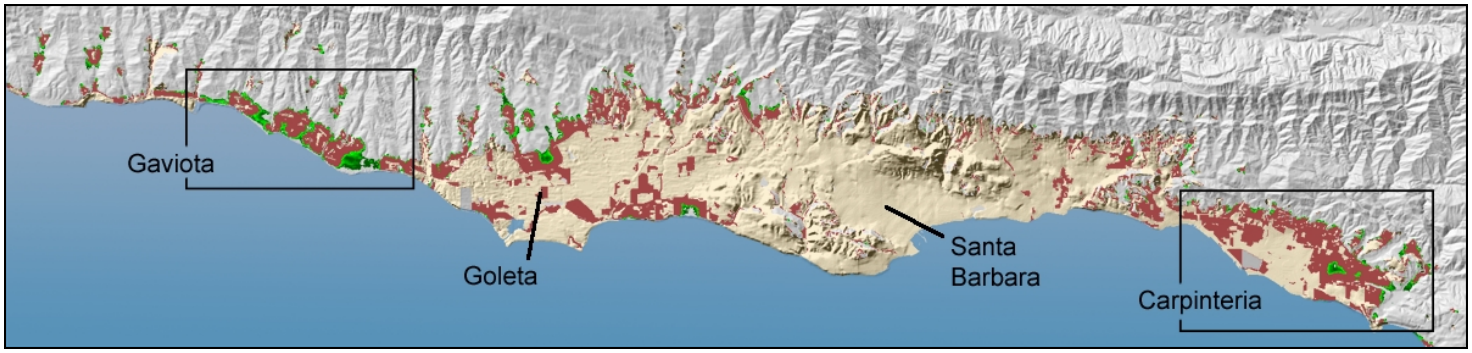

Figure 6-32: Recent_data urban probability forecast for the year 2030

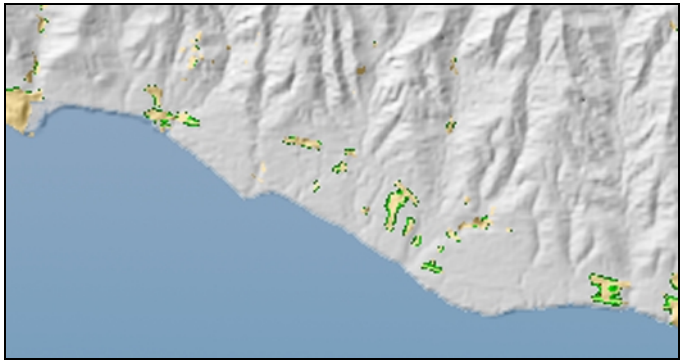

Figure 6-33b: detail of All_data 2030 forecast of the Gaviota area

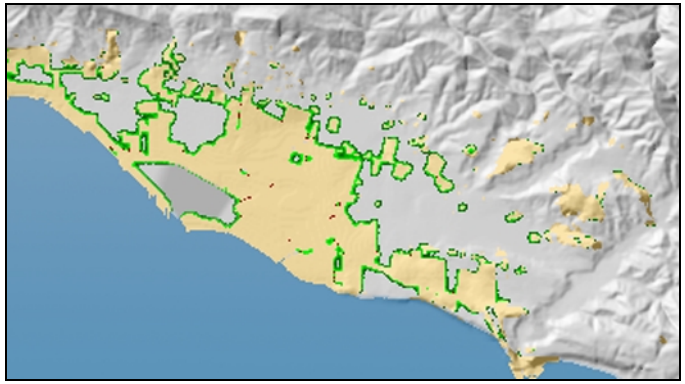

Figure 6-33a: detail of All_data 2030 forecast of the Carpinteria area

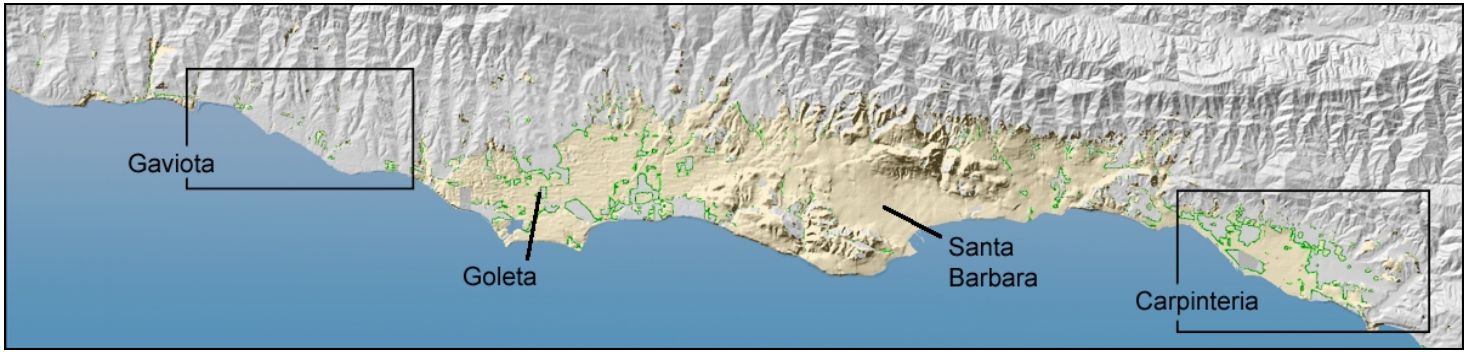

Figure 6-33: : Sparse_data urban probability forecast for the year 2030

6.2.3.1 All_data

The All_data scenario forecasted that over 60,000 currently non-developed 30m pixels will be urban by the year 2030 with a probability of 90% or greater (Figure 6-31). With a very high degree of probability, urbanization spread across most of the available land with moderate topography, especially evident in the area around Carpinteria (Figure 6-31a). Development also followed Hwy 101 West of Goleta, along the Gaviota Coast (Figure 6-31b). Mild development spread into the gently sloped canyon areas North of Goleta and outside of Carpinteria. Moderate in-filling in Goleta and Carpinteria was forecast, but a substantial area East of Carpinteria is still shown as open land.

6.2.3.2 Recent_data

The Recent_data scenario, with over 52,000 non-developed 30 m pixels forecasted as urban in the year 2030, produced the most aggressive forecast of urban growth (Figure 6-32). The importance of urban-infilling in this scenario is illustrated in 6-32a. All of the available flat land, most of which is surrounded by already urbanized lands, has a greater than 50% probability of urban development. Importantly, a large majority of these transitions are forecasted with a probability of 90% or greater. Outward or edge growth also played a large role in this application. In the areas north of Goleta and along the Gaviota Coast (Figure 6-32b) high probability urban transitions spread outward from existing urban settlements. The lesser affect of road-influenced growth in this scenario is also illustrated in (Figure 6-32b). Moderate to low probability urbanization surrounds both Hwy 101 and Cathedral Oaks Road, (a

primary transportation route) between existing- and high-probability urban centers. The Recent_data scenario forecasted growth in the foothill areas as topography allowed.

6.2.3.3 Sparse_data

The Sparse_data scenario produced a virtual "no growth" forecast for the South Coast Region (Figure 6-33). In the over thirty growth cycles applied to the input data, less than 900 30 m pixels were forecast as urban transitions with a probability of 90% or greater. Most of this development occurred as infilling in the most densely urban spaces. The remaining portion of highest probability transitions occurred at the immediate edge of currently existing urban areas. The other four probability classes averaged about 2200 pixels each. These transitions were also attached to currently existing urban areas with the highest probabilities being the closest to current settlements and descending as distance from the settlements increased. Growth was so minimal that roads and slope had no evident effect.

6.2.4 Forecast Difference Maps

In a GIS values of 50 or greater from unclassified probability values (that ranged from 0 to 100) were selected from each forecast map (Figure 6-34 – Figure 6-36). These maps were then compared by subtracting one map (the first) from another (the second). The resultant maps values give spatial context for the difference of forecasted probabilities. A value of 0 at a location indicates agreement between the first and second maps, or two forecasts. The larger the value, the greater the first forecast "over estimated" urban growth with respect to the subtracted map. Similarly, a large negative number indicates urban probability favored by the second forecast

map. The values were grouped into decadal classes and color classified in grayscale from 0 – 255.

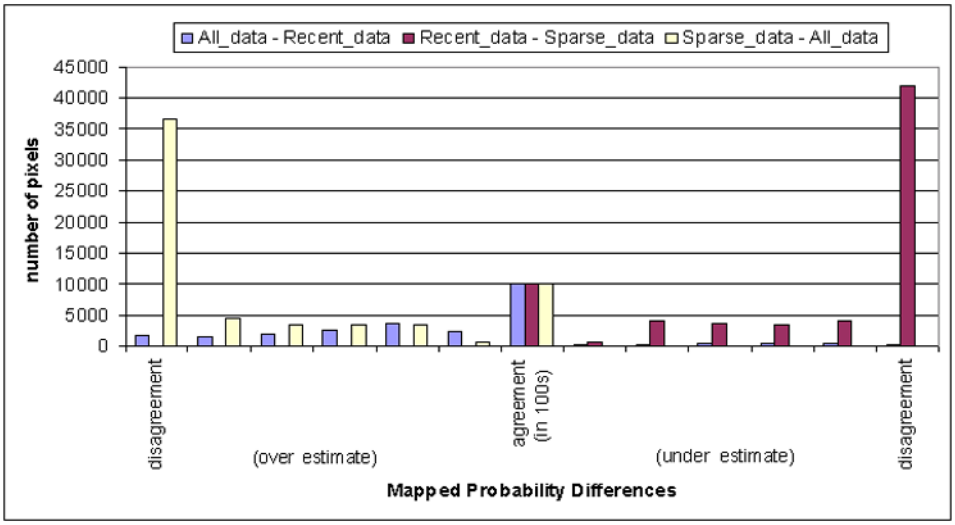

Figure 6-34: Per class pixel count for the forecast difference maps

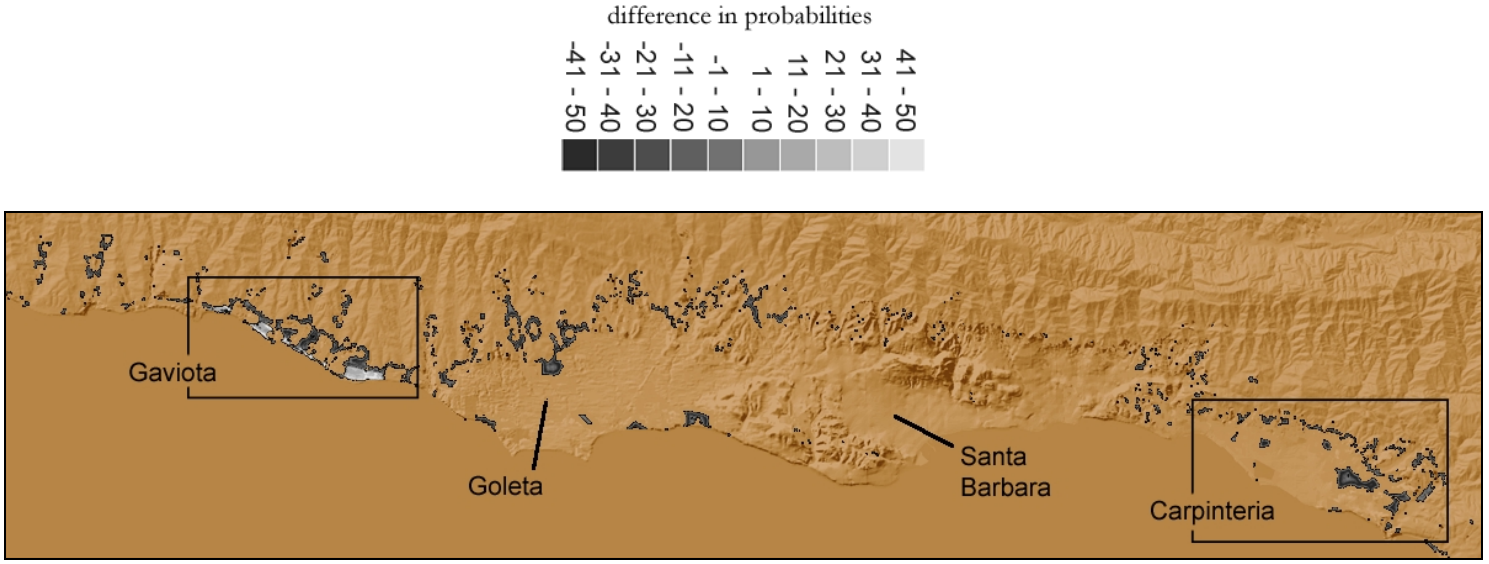

Figure 6-35: 2030 All_data - Recent_data difference map

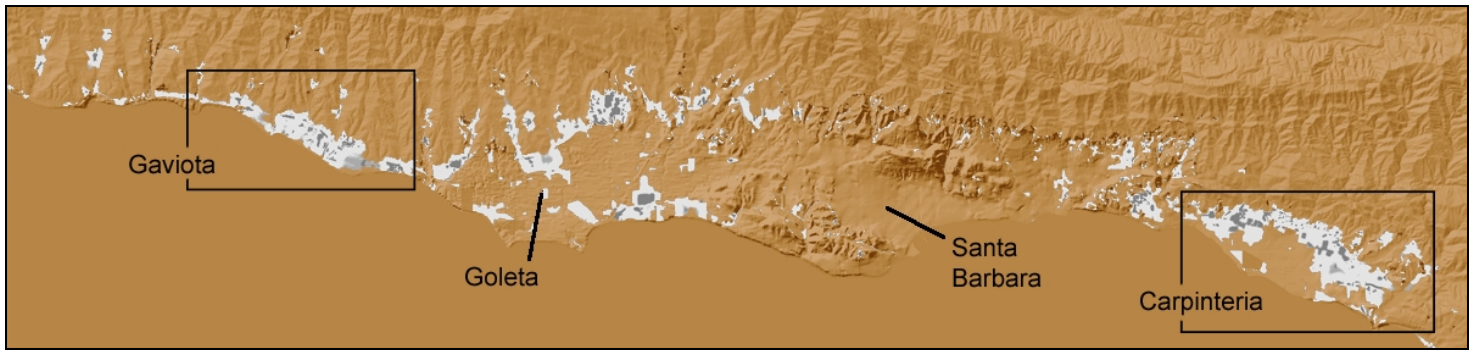

Figure 6-36: 2030 Recent_data – Sparse_data difference map

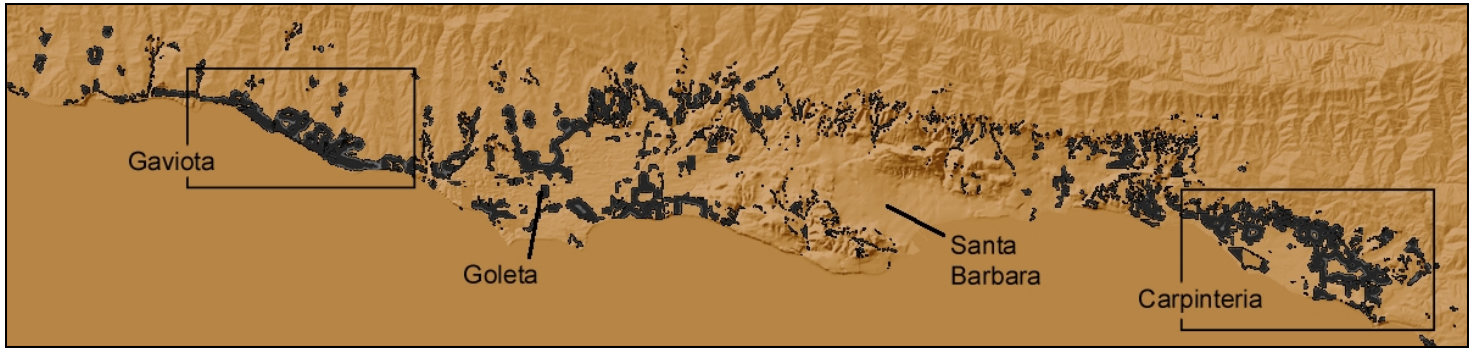

Figure 6-37: 2030 Sparse_data – All_data difference map

6.2.4.1 All_data – Recent_data

Figure 6-35 illustrates Recent_data's aggressive edge growth shows as overestimates on the urban fringe areas throughout the region. Also, topography appears to be more of a constraint in the All_data scenario, as Recent_data contains more urban transitions in the steeply sloped foothill areas. The strong affect of Hwy 101 in this scenario can be seen in the agglomerations of dark cells in the Gaviota area (Figure 6-35b) that hug the highway route along the coastline.

6.2.4.2 Recent_data – Sparse_data and Sparse_data – All_data

The number of transitions in the Sparse_data scenario was so few that the comparisons with All-data (Figure 6-37) and Recent-data (Figure 6-36) essentially read like mirrors of the comparison maps. Probability differences located immediately adjacent to currently urbanized lands have slightly lower values than the probabilities of All_data or Recent_data alone, but this is the only significant patterning, which is at best negligible.

6.2.5 Computational Time

The amount of required computer processing unit (CPU) time is of great concern to model calibration. SLEUTH methodology, in an effort to minimize this overhead, implements hierarchical brute force calibration. Additionally, since a true parallel processing environment was not available for this research, calibration jobs were run in a pseudo-parallel environment as described in Section 5.5.1. Each calibration job

was divided and delegated to shared workstations. The timings for each of these jobs were assembled and are displayed by scenario and execution phase in table Table 6-2.

	Scenario					
	All_data		Recent_data		Sparse_data	
Phase	hours	coef sets	hours	coef sets	hours	coef sets
Coarse	285.45	3125	93.23	3125	218.98	3250
Fine	342.15	3600	79.28	3125	133.28	3000
Final	353.62	3000	96.75	3750	232.27	4500
Derive	8.80	1	1.95	1	6.32	1
Predict	4.75	1	2.90	1	2.33	1
Total	994.77	9727	274.12	10002	593.18	10752
average time: (in minutes)		6.14		1.64		3.31

Table 6-2: Computational time required for SLEUTH calibration and forecasting

All_data required largest amount of CPU time (almost 995 hours) for all phases of execution, with an average time for a single simulation of 6.14 minutes. Sparse_data required only 593 hours (average single simulation time 3.31 minutes), even though the same number of growth cycles (from 1929 – 1998) was required for both runs. Recent_data, with 32 growth cycles, needed roughly half of Sparse_data's requirement at 274 hours and an average single simulation time of 1.64 minutes.

Chapter 7

7 CONCLUSIONS

7.1 Temporal Input Efficacy for Calibration and Forecasting

This research was driven by the lack of knowledge regarding the calibration of urban CA models. In order to add information to the fields of urban and land use modeling, CA modeling, and complex and dynamic system modeling, an examination of an urban CA (SLEUTH) to test calibration sensitivity to temporal controls was performed. The null hypothesis guiding this work was: The duration and number of years used as controls for calibration of SLEUTH in the Santa Barbara study area will have no affect on the calibration results. To prove or disprove this statement three separate calibration scenarios were run, each achieving different measures of success (Figure 6-6 - Figure 6-11). It was found that by varying the density or temporal duration of the control data, calibration scores were affected and the number of control years used in calibration does make a difference. Further, the second scenario, Recent_data, consistently performed the best in calibration, given the ranking and sorting methodology used in this application.

Recent_data's product scores were much higher through the three phases of calibration (Figure 6-6) than the other scenarios. The Recent_data calibration utilized the four most recent temporal images (from 1967-1998) to initialize growth and generate regression scores, as opposed to the other two calibrations that initialized in 1929. Recent_data consisted of short-term, high-density historical data. Therefore, for

this application, the forecasts from a short-term, high-density calibration can be given a greater degree of certainty for short-term forecasting than a calibration using older, long-term data, even if several more control years are added to the long-term database.

This finding – that a temporal database of 33 years most accurately calibrated urban change for the study area – benefits urban model calibration in four ways. First, the time required to generate the urban input layers will be greatly reduced. The further back in time from the present a temporal GIS database reaches, the more difficult it is to locate and assemble accurate data layers. Often different products, such as aerial photography and hardcopy maps, from various sources need to be used. These data often exist in formats that are time consuming to enter into a GIS acceptable format. Using data available from the mid-sixties to the present to calibrate urban change, as Recent_data did, minimizes these time consuming tasks. For most regions in the United States, and many other parts of the world, four or more satellite or aerial photographic images from the last three decades can be acquired to accurately calibrate urban change.

The second benefit of short-term calibration is the older data-source products often use different methods of classification that can make consistency between data layers difficult, if not impossible. The further back in time the historical layers go, the greater the uncertainty regarding their accuracy. The classification of modern data will be more consistent than relying on aged hardcopy maps and other forms of historical information. Third, complete coverage of large areas, especially for one time period, is

often difficult to find for older dates. Satellite data sources provide a greater probability of providing continuous, consistent datasets that cover large areas over several time periods, enabling regional modeling as opposed to only city or county based.

The fourth benefit from the success of Recent_data pertains to the computer requirements associated with calibration. For computational models that require a great deal of computer processing units (CPUs) for calibration (such as SLEUTH) any reduction in the number of years that a region must be calibrated for is valuable. While there must be some minimum number of years that must be simulated in order for a calibration to be valuable, it can at least be said that 33 years is better than 69. For the South Coast that means cutting the CPU time required for calibration by at least half.

While the benefits listed above are clear contributions this research provides, the geographic and historical profile of the South Coast presents a particular urban growth profile. Santa Barbara's limited potential for continued growth due to geographic limits and specific urbanization pressures dictated calibration, and of course play a role in the generalizability of these results to other SLEUTH applications. Areas with less topographic constraints or waning growth pressures might derive alternative conclusions. However, many costal or mountain communities with a history of attacting growth will certainly find these results quite applicable.

It also must be noted that a calibration with fewer control points will tend to produce higher r^2 values simply because there are fewer data points to fit. A trade off occurs

between the robustness of a historical profile, and a less successful regression score due to increased variance. This could be why the Sparse_data scenario performed so much better than the All_data scenario, but produced a forecast that could not possibly represent Santa Barbara's future urban growth. All_data, on the other hand, produced a more believable forecast, that is also similar to Recent_data's. Though Sparse_data and Recent_data each used four control years, Recent_data maintained a higher product score than the Sparse_data scenario for calibration. It could be that the duration of time *between* control years is more significant to a good calibration than control year density, or the period of time over which the calibration occurs.

7.2 Calibration Metric Effectiveness

The population metric is a completely non-spatial measurement and was the easiest curve to fit for calibration. Population regression scores for all calibrations were greater than 0.92 and final calibration scores were all above 0.95. The average number of urban edges, average number of clusters, and average cluster size are peripheral attempts to quantify the spatial structure of urban growth. These measurements showed variation in their scores across the calibration phases and in most cases did not consistently improve or decline in performance. Even so, these regression scores achieved 0.85 or better by the final phase, with the exception of All_data's edges metric witch leveled off at r^2=0.78. It is especially difficult to achieve high performing results with the Lee Sallee metric so 0.47 is considered a fairly good fit. Recent_data's best score was r^2=0.70, and All_data and Sparse_data never did better than 0.47.

However, the Lee Sallee is vital as an indicator because it is the only explicitly spatial metric implemented by SLEUTH.

For this application, calibration metrics were ranked using the product of five evenly weighted metrics. These five metrics gave an indication of how well SLEUTH simulated urban change for the South Coast, but were found to be lacking in a few ways. The large disconnect between calibration and forecasting values calls into question how well future growth is being simulated. Figure 7-1 was created by graphing Figure 6-3 and Figure 6-24 together, and shows the continuum of metric behavior from historical through forecasted change.

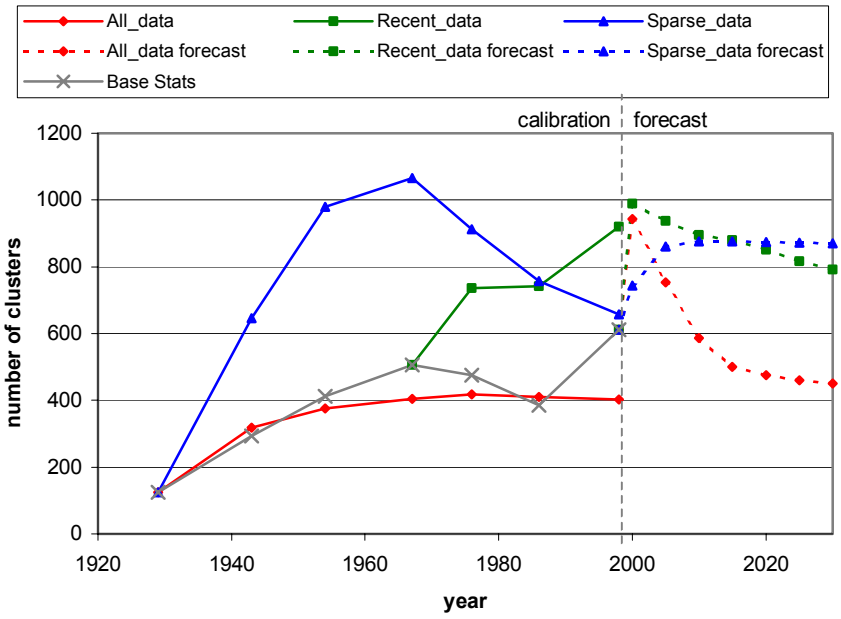

Figure 7-1: Average number of clusters for calibration and forecasting

An especially confusing instance is illustrated by graphing the average number of clusters over the processes of prediction and calibration (Figure 7-1). The erratic

behavior of this metric during the first years of forecasting is unusual, but exemplify the kind of disconnect that occurs when the simulation is initialized with new data between the calibration and forecasting phases. The introduced seed year is so different than the simulated configuration that the types of growth can change radically when applied to the new environment. This variable behavior demonstrates the adaptive qualities of CA to current lattice conditions, but does little to encourage faith in the calibrated solution set for forecasting. The *compare* metric is a measurement of the final control year population compared to a simulation's population count in the final year. Such a metric emphasizes the state of the "current" urban extent in simulation success. Including the compare metric, or others like it, into the product score could minimize this problem. By rewarding runs that simulate current conditions in addition to historical change especially well, transitioning between calibration and forecasting will be less abrupt. It is not clear from this work if one or a set of the metrics should be given precedence (weight) over the others, or that one metric is any more useful from the others used. Not knowing which or in what combination to use various metrics is a great difficulty of calibration, and a limitation to urban CA efforts. By graphing simulated metric values against the base statistics (Figure 6-7 - Figure 6-11), and considering their related regression values, other limitations of the metrics are revealed. Using the population metric as an example (shown below as Figure 7-2), it would appear that of the three scenarios, Recent_data's values are closest to the base statistics.

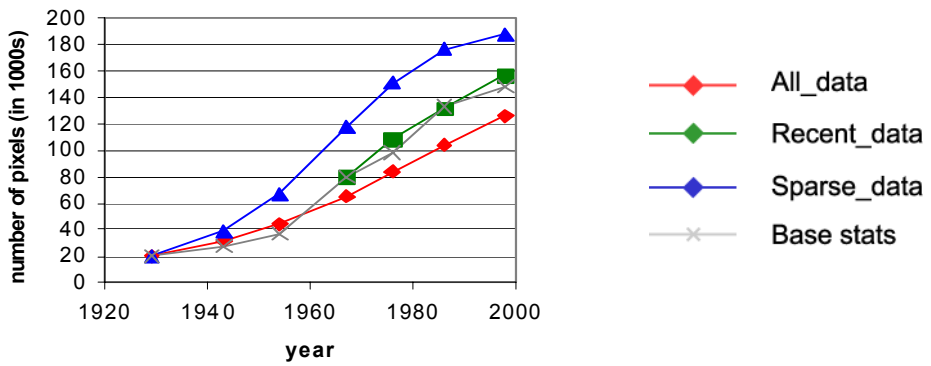

Figure 7-2: Population metric for calibration

However, All_data has a regression score of 0.97, while Recent_data's score is only 0.95. By using only the linear regression score to grade simulation metrics, the trend rather than the actual metric values are being rated. This can result in a coefficient set that misses the base statistic values by a large but constant quantity, outscoring another set whose values are closer to the control data, but whose trend is off. This occurs because the shape of the line is being rewarding without respect to its context. As a response to this, measurements of the offset and slope of the line, instead of only the line itself, should be used to characterize metric behavior.

7.3 Coefficient Behavior

Using data written to the `avg.log` file during the derive and forecasting runs, a detailed view of coefficient behavior was generated. Using these data, the critical system wide phase changes of boom and bust can be identified. Each of the derived coefficient sets followed the same pattern of exhibiting a boom state for a period of time, and then entering a bust state until the completion of the simulation. Because more than one coefficient affects each growth rule, it is difficult to establish a direct

relationship between the metric and coefficient values. In general, the metrics (Figure 6-7- Figure 6-11 and Figure 6-22 - Figure 6-25) increase in rate or actual number more rapidly in the first half of the run and then decrease or decelerate in the second half, a trend that corresponds with the coefficients' boom and bust states. However, with the exception of Sparse_data, the onset of the bust state did not match the timing of the South Coast's rate of urban expansion. The population count for the base statistics (Figure 6-1) shows a large boom period between 1954 and 1967 and a smaller one from 1976 – 1986, with slowed growth between these periods. From these results it appears that the self-modification values inherited from calibration of the Washington-Baltimore at 120 m are not appropriate for application to the South Coast data. This is not entirely surprising since the scale and development history of the two areas are very different.

The minimum and maximum limits of the coefficients have an effect upon coefficient dynamics. In the coefficient graphs for calibration (Figure 6-17 - Figure 6-21) and forecasting (Figure 6-26 - Figure 6-30) it can be seen that for long periods of time coefficients are forced into static values due to these limits. The breed coefficient in All_data for example remained at a value of 100 for 72 out of 101 years of simulation. Given a period of time and a constant self-modification state (e.g.; boom) several coefficients may reach a limit, but at different times. When the self-modification state changes (e.g.; from boom to bust) these coefficients will be adjusted from an identical value, in the same time period. (See breed and spread coefficient values for All_data and Sparse_data). The persistence of the coefficients at limit values, coupled with the

self-modification rules, enforces what could likely be an unrelated correlation between coefficient behavior. Additionally, these limits maintain a static coefficient value in a still dynamic system. A modification of the self-modification functions so that these limits are not reached so quickly would lessen these problems.

The different brute force calibration paths taken by each scenario are illustrated in the coefficient solution space graphs (Figure 6-12 - Figure 6-16). While coefficients within a scenario occasionally narrowed immediately to a small range (The All_data and Sparse_data dispersion values shown in Figure 6-12 for example.) none of the scenarios or coefficients exhibited a particular ease in identifying a set of best-fit values. This shows that none of the scenarios had a particular time saving benefit of quickly identifying best-fit coefficients without going through the three phases of calibration.

Most applied cellular models are constrained to generate particular numbers of cells in each state, with the target cell numbers determined exogenously, usually by another model (White and Engelen, 2000). In contrast, SLEUTH allows the simulated city to evolve without growth restrictions. Urban forms emerge solely from the configuration of the initial conditions and application of the transition rules, which is a strength of the model. However, it assumes that the study area is a closed system, which it is not.

7.4 South Coast Forecasts

SLEUTH3.0 was successfully calibrated to the Santa Barbara study area at the local level using 30m data using three different calibration scenarios. Each scenario generated a unique BSS that was used to initialize forecasts of urban growth from 1998 to 2030 (Figure 6-31 – Figure 6-33). Even though the BSS for All_data and

Recent_data were quite different, their forecast maps for 2030 are similar, especially when compared with Sparse_data's "no growth" forecast.

Recent_data produced the most aggressive new growth forecast of the three forecast scenarios. Most of the newly urbanized pixels were transitions from outward growth at the urban edge. The number-of-urban-pixels graph (Figure 6-22) shows that All_data and Recent_data supported similar urban growth rates until the year 2015, when they begin to diverge. At this point in time both scenarios enter into a "bust" phase. The spread and breed coefficients for All_data (Figure 6-28) drop sharply, and the population quickly flattens for the remainder of the simulation. The same values for Recent_data however, decrease at a more moderate rate. The reason for this very different reaction between scenarios is not clear, but illustrates the importance of self-modification to simulation evolution and reiterates the importance of this behavior to modeling dynamic urban systems (Clarke and Hoppen, 1997; Clarke et al., 1997; Silva and Clarke, forthcoming).

The sluggish urban growth produced by the Sparse_data forecast is also a result of coefficient self-modification. The bust state entered into after 1986 caused a crash in coefficient values that the system could not recover from. At the initialization of the forecast runs, the very influential spread coefficient values of All_data and Recent_data were both 100. The spread_coefficient value of Sparse_data was only 38. The other values in Sparse_data's BSS were not enough to encourage growth upon commencement of the forecast run. The pattern of Sparse_data's coefficient bust is not unlike that experienced by All_data in the forecast period after 2015 that had the

same affect of leveling off the growth rate. If the self-modification parameters would have been calibrated for this scenario, the affect of the critical bust could have been lessened. Sparse_data was calibrated using four control years with an average difference of 22 years between each data point. The fact that this scenario's best calibration score was produced from a simulation that generated a fatal bust to the system further illustrates the duration of time between control years is of great importance to a "believable" calibration.

The importance of transportation system development to urbanization dynamics is illustrated nicely in the All_data and Recent_data scenarios. In the early period of Santa Barbara's development primary transportation systems played an important role in carrying new growth east and west from the city center. Through calibration, the All_data scenario captured this dynamic by selecting a high road_gravity value. The resultant road_gravity coefficient selected by Recent_data, however, was relatively low. By the mid-sixties to present most primary roads were already surrounded by urban infrastructure and a preponderance of new development claimed lands at the suburban edge instead of escaping along major transportation routes. Emphasizing road gravity influences in such a scenario did not benefit the calibration. These calibration behaviors carried through into the forecast simulations and are illustrated in Figure 6-31b and Figure 6-32b. In the All_data forecast (Figure 6-31b) the curvilinear pattern of high probability growth along the coast follows Hwy 101, the major highway through the South Coast area. Recent_data's emphasis on growth from the urban edge instead of routes of transportation produced clustered organic

growth around urban settlements (especially in the 95 – 100% probability range) with lesser probability transitions occurring with equal likelihood along Hwy 101 and primary roads.

The road_gravity coefficient for Sparse_data was lower than of All_data's, but higher than Recent_data's throughout historical simulation. It could be that the road_influenced growth from the early control years of the Sparse_data scenario (1929 and 1954) were not of great enough affect compared to the large amount of organic growth that occurred by the next control year (1976). As with the Recent data scenario, edge growth took precedence and Sparse_data selected a very high spread coefficient and only a moderate gravity coefficient.

In addition to calibration, the quality of model prediction or forecasting may be seen as a function of the degrees of freedom defining the solution space. When a model is executed on a homogenous, infinite plane, as is the case with a formal CA, any growth pattern is, in principle, possible. In such an instance, generating the correct future state of a system from an initial configuration gives a very high degree of confidence in the model's predictive ability. As model constraints are added (exclusion layers, topography, etc.) the number of possible growth patterns is drastically reduced, and the value of the prediction is accordingly reduced. In the case of the South Coast there exists the additional constraint of limited available space for new urban development. This aerial limitation influences prediction so that the number of possible growth patterns is also reduced over time. At the limit, any model will predict the correct pattern if there's only one place for growth to occur. This is perhaps why

the All_data and Recent_data forecasts are so similar. The real value of a predictive model is the *unexpected* knowledge it provides. The predictive goodness of a model may decrease as the time passes simply as a function of system entropy. This could be seen as a limitation of the study area as much as the model.

7.5 CPU Usage

Table 6-2 lists the number of computer processing hours required to complete this work. The total computational time spent by each scenario is not directly comparable because the total number of simulations completed by each scenario varies due to increment values used for brute force calibration. These total-values were normalized by the total number of simulations per scenario. Not surprisingly, the Recent_data scenario required the fewest hours because the number of growth cycles per simulation was only 32, compared to 69 growth cycles per simulation for All_data and Sparse-data. With the same number of control years (4), Sparse_data's average simulation time at, 3.31 minutes, was roughly twice that of the 1.64 minutes used by Recent_data. What was surprising was how much overhead the three additional control years would add in increased statistical computation. At 6.14 minutes, All_data required almost doubling the time used by Sparse_data due to calculating calibration statistics for three additional periods.

Chapter 8

8 FUTURE WORK

The urban dynamics SLEUTH simulates, and calibration attempts to capture for a specific study area, are general to urban growth patterns: over time urban areas amass more land, spread out from urban edges and in independent settlements, are attracted to routes of transportation, and are resistant to steepening terrain. While many lessons learned from this research can be directly applied to our specific methodology, they can also be transferred to the more general problems of calibrating dynamic system models, specifically CA models representing urban and land use transitions.

8.1 Scaling Influences

The testing of scaling influences upon brute force calibration methodology was carried out as a precursor to temporal sensitivity testing. It was found that while SLEUTH itself is scalable, in that it can be effectively applied to different urban systems at various scales, the process of calibration is not. The process of resampling control data for calibration can actually exclude the optimum coefficient set selected by the full resolution data. While (Silva and Clarke, forthcoming) illustrated interesting findings regarding urban characteristics revealed by examination of coefficient behavior between different resolutions during calibration, it could well be these results are "reminiscent" of urban dynamics rather than capturing real scaling processes. Continued research on the dynamics of urban systems at multiple scales will shed light on these initial findings.

8.2 Intra-period Duration

Through this research the trade-off between a high statistical calibration score and a more robust (and even believable) calibration is evident. Sparse_data is an excellent example of how something can go wrong with a good calibration method. The model was fit to the historical data, and had a much better score than the All_data scenario, which covered the same historical period. However, the "great depression" of coefficient self-modification at the very end of the calibrated simulation "busted" the system and made the forecast solution set ineffectual to generate continued urban transitions. The large amount of time between control points allowed for extreme system shifts (beyond what was found in the control data) that did not negatively affect in a significant way the calibration's final score.

While the need for greater control and calibration of CA self-modification parameters is evident, in order to avoid such unexpected behavior in calibrated results, an average intra-control year duration of 23 years (that of Sparse_data) should be considered a maximum for historical calibration. A shorter intra-period duration of ~11 years (that of All_data and Recent_data) can at least be recommended, as both scenarios produced forecast results that seemed reasonable for short-term prediction. However, if calibration data is only available with long duration periods, mapping the behavior of metric and parameter values using the methods introduced here is critical to a) avoid selecting a coefficient set that allows a terminal system crash, and b) inform forecasting results by illustrating historical behavior.

8.3 Calibration Duration

The short-term, high-density scenario executed in the Recent_data application has advantages over the long-term, high density scenario of All_data in two primary ways. First, Recent_data's overall performance score was better than All_data's. However, it is possible that a high-density calibration with fewer data points will always return a better score because of fewer points to fit. Additional research will shed light on this affect. Second, assembling and calibrating a short-term temporal GIS is less costly, and more reliable in terms of time, dollars, and accuracy. This second point offers enough benefits in decreased cost to make the short-term, high-density calibration more preferable than the long-term, high-density scenario.

8.3.1 Long-term calibration for long-term prediction?

In defense of the All_data scenario it could be argued that the longer historical calibration will provide a better basis for long-term forecasting. This argument stems from our knowledge of events in the past and future. The state of being that we can be most certain of is the present. The further away from the present a given state is known the greater the uncertainty regarding that information, simply because time has passed, allowing for state change to occur (Figure 8-1). Similarly, if a prediction is made, the further into the future something is described, the less certain we are of the prediction proving to be accurate.

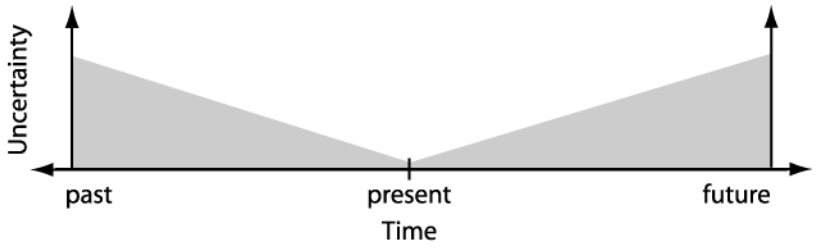

Figure 8-1: Graphic representation of the temporal relationship of uncertainty

Though imperfect, historical databases provide placeholders of previous conditions. These "reality points" act as anchors for historical simulations and help minimize the uncertainty associated with past states. An accurate calibration of the dynamics that influenced a system's past provides more knowledge about that system than its current state. With the knowledge of system dynamics provided by calibration, the uncertainty regarding a system's future state can be reduced (Figure 8-2). So perhaps profiling a longer history during the calibration process will capture a richer range of behavior, and provide a better source for forecasts that range far into the future (Figure 8-3).

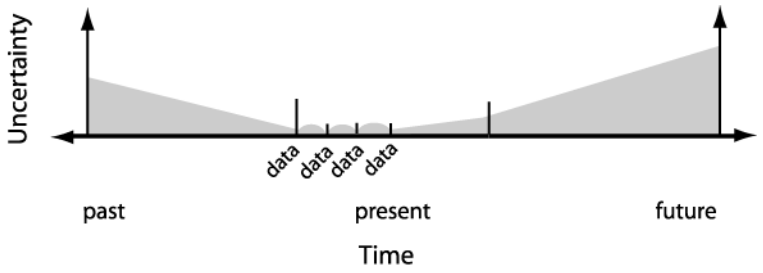

Figure 8-2:Graphic representation of the temporal relationship of uncertainty when short-term data is added. Note how, in the future, after the temporal period for which calibration was performed has been surpassed, the uncertainty is no longer reduced.

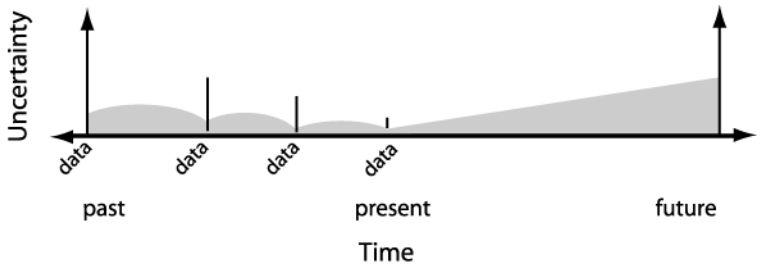

Figure 8-3: Graphic representation of the temporal relationship of uncertainty when long-term data is added. Note how uncertainty in the future is reduced for a longer time than when short-term data is used for calibration.

8.4 Trend Characterization

There is a difference between best generating a present condition from some former state, and accurately simulating a trend. The possibility that the best calibration was derived from the most recent data could be a coincidence of data collection, and not necessarily the best representation of the South Coast's historical growth dynamics. The finding that the most recent data best characterizes present day Santa Barbara makes intuitive sense: a composite of an individual's portrait photographs from the past ten years will look more similar to his/her present condition than a composite of pictures from infancy to adulthood. Similarly, we derive the best simulation of an urban area's morphology to a current state by modeling its most recent change, instead of a longer history. However, this reasoning is only appropriate if change is more or less linear. (As is assumed in the hypothesis presented in section 8.3.1). If rapid change occurs over brief periods of time, the linear assumption breaks down and will not be able to accurately describe the growth *trend*.

The task of calibration is to identify and reproduce properties of a multi-dimensional space that best represent an actual urban growth trajectory with the greatest amount

of efficacy. If there are significant non-linearities in this trajectory, the timing and spacing of control data points becomes critical to the curve-fitting methodology. This leads back to the issue of density and duration in the control data series and the question: are the temporal properties of growth being captured, or is an important cycle falling through the cracks? Since SLEUTH is a trend extrapolation model, the quality of its predictions depends heavily on (a) how well calibration was able to capture the trend, and (b) how smooth that trend is for the particular urban area. As these historical trends can only be discerned from the amount of data available, it is a bit of a chicken and egg problem. However, as accurate spatial data becomes ever more available at smaller temporal intervals, these issues can be explored more fully.

8.5 Calibration Metric Effectiveness

The subset of metrics used in this application successfully calibrated the model to the data. However, limitations to their efficacy were found. By only using 5 metrics, instead of a possible 11, the process of describing *why* a particular simulation performed better than another was simplified. However, the inter-related behavior of the coefficients and metrics is still complicated, and it is not clear from this work if one or a set of the metrics should be given precedence (weight) over the others, or that one metric is any more useful from the others used. What was found is that a need to create a smooth transition from historical simulation to forecasting will greatly improve the believability of forecasted results. To that end, metrics that reward accurate prediction of present conditions during calibration are recommended. Not knowing which, or in what combination, to use various metrics, is a great limitation to urban CA calibration. Testing the ability of metrics to capture spatial patterns and defining their relative

importance will streamline calibration efforts and bring more confidence to forecast results.

Additionally, by using only linear regression scores to grade simulation metrics, the trend rather than the actual metric values are being rated. What this can amount to is a coefficient set that misses the base statistic values by a large, but constant, quantity may outscore another set whose values are closer to the control data, but whose trend is off. This occurs because the shape of the line is being rewarding without respect to its context. As a response to this, measurements of the offset and slope of the line, instead of only the line itself, should be used to characterize metric behavior.

8.6 Portability of Self-Modification Values

The boom and bust states involved in SLEUTH's self-modification behavior had very important influences on simulation results. However, these state changes missed the periods of boom and bust experienced by Santa Barbara in both time and scale. It follows that calibration success could be greatly improved by calibrating self-modification values for a data set. The basic self-modification values applied in this research were inherited from calibration of UGM1.0 (a previous version of the SLEUTH urban growth model) to the Washington-Baltimore area. The Santa Barbara temporal GIS is very different than that used to calibrate Washington-Baltimore in both scale and temporal duration. These differences alone might have been enough to determine the non-portability of self-modification values. However, several changes in the influence of coefficient values upon the transition rules in SLEUTH v3.0 make it very likely that the influences of self-modification values do not have the same affect

as in previous model versions. With six additional variables, calibration of these self-modification values will increase CPU time substantially. However, new theory or methodology could lessen this additional overhead.

Here, modification of SLEUTH brute-force calibration methodology is proposed: The best product scores for each of the scenarios did improve through the phases of calibration (Figure 8-4). However, how significant the improvement was, is uncertain.

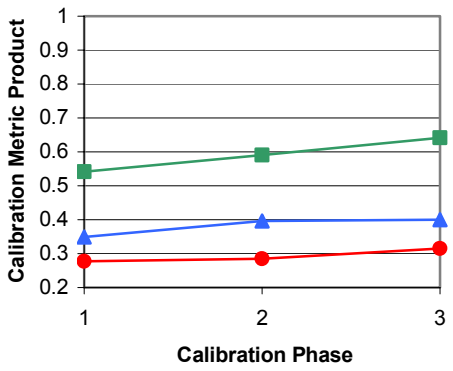

Figure 8-4: Product score of calibraton metrics for each scenario

Derive and forecast runs can be performed on the best coefficients selected from coarse calibration and final calibration phases. It might be found that the calibration and forecast produced in the coarse phase generates satisfactory results, especially when the trade-off in saved CPU time is considered. Additionally, a greater degree of improvement might be achieved by refining the self-modification values. To test this hypothesis, a coarse calibration, without self-modification, could be executed. From this run, the best performing coefficients are selected and held as constant. Using this set of coefficients, a coarse run through the self-modification values would be

performed (Limits to values would have to be decided). Would the results be better than the three phases of calibration of the behavior coefficients? If this methodology is effective both behavior coefficients and self-modification parameters are calibrated for a data set, simulation accuracy is improved, and the amount of CPU required for calibration has not been increased.

Alternatively, the portability of SLEUTH v3.0 self-modification parameters could be tested. This examination could be performed in two ways. A robust calibration of SLEUTH v3.0 self-modification values for a region could be performed and then applied to another data set. In such a case the parameters from the previous data set might prove sufficient for other applications. A more empirical approach may be taken, and is described in more detail in Section 8.7.2. By studying the patterns of boom and bust in temporal GIS databases, theory about the dynamics of these phase changes can be developed and implemented in model self-modification behaviors. While the parameters that of such implementation would still require fine-tuning for an individual data set, the underlying functionality is defendable and more transparent than its current realization.

8.7 Pseudo-parallel Processing

While not a perfect system, the pseudo-parallel processing calibration methodology was very useful to the completion of this work. 30,000 CPU hours were required to calibrate and forecast the three scenarios. By dividing up the scenario into parts and assigning the job to one of 14 workstations, the actual time required for calibration was only one tenth of the total CPU time. The configuration, while infinitely helpful, did have its problems. The workstations were in an open lab. Since lab use during the

execution of this research was low (summertime) the machines were generally completely available for calibration applications. However, if even one additional job was started up (e.g.; Netscape), the CPU was immediately cut in half for the calibration job. This caused some uneven timing in the completion of phases, but didn't effect the results (unless a workstation was shutdown, in which case that job would be re-initialized.)

8.8 Urban CA Dynamics

8.8.1 Theoretical examination

A criticism of urban CA models is that as the formal rules are relaxed, the dynamics of the model become more difficult to understand and results become less clear. This study found the inter-relatedness of SLEUTH coefficients in the application of the transition rules, and the dynamics of self-modification may mimic the complex dependencies of real urban systems, but muddles the description of the underlying dynamics. Describing the relatedness of coefficient values to metric behavior is difficult, especially in the context of a complicated urban system. Starting with the transition rules SLEUTH proposes, how well real urban processes (road attraction, new spreading centers, slope resistance) are modeled in a theoretical environment can be investigated. The previous (and current) research efforts of SLEUTH have been application centered. However, a more theoretical examination of the model functions can describe and explain behaviors generated under the simplest conditions. Lessons learned from such work would have at least two immediate benefits: 1) it will lead to the illumination of simulation dynamics on more complex or "real" data 2) Results

could indicate simplifications of the transition and self-modification rules that would lead to greater transparency of coefficient application effects.

8.8.2 Real world dynamics

The U.S. Geological Survey's urban dynamics program has compiled temporal GIS databases for urban systems all over the country. Study regions include San Francisco–Sacramento, Portland-Seattle, Middle-Rio Grande, Detroit-Chicago, and Chesapeake Bay. These databases contain the historical information that SLEUTH simulations use as controls for calibration of urban growth dynamics. By applying the methodology of mapping metric values for historical databases that was introduced in this research, a cross regional study of these databases to examine their behavior will provide a testing set to examine urban theory, and produce new theories about the evolution of urban structure.

For example, Zipf's Rank-Size Rule defines the log linear relationship between city population and rank. Using the temporal GIS databases, the Rank-Size rule can be applied to urban area instead of population, and studied across scales and over time. Results from this research will increase knowledge about the evolution of urban spatial patterns over time, and can inform, or even serve as a measure for geographic models of urban dynamics. "The importance of (Zipf's) law is that, given very strong empirical support, it constitutes a minimum criterion of admissibility for any model of local growth, or any model of cities" (Gabiax, 1999).

The persistence of the coefficients at limit values, coupled with the self-modification rules, enforces what could likely be an unrelated correlation between coefficient behaviors. Additionally, these limits maintain a static coefficient value in a still

dynamic system. A modification of the range so that these limits are not reached so quickly would lessen these problems.

Additionally, by examining how the structure of urban systems evolves historically, new hypothesis of urban evolution may be developed. For instance, in the Santa Barbara historical data, the number of clusters increases in the early part of the data set, begins to decrease, and then displays a sharp increase. The trend of this metric could describe a pattern of cyclic behavior regarding urban cluster size over time. This examination of temporal cycles could lead to additional hypotheses about the nature

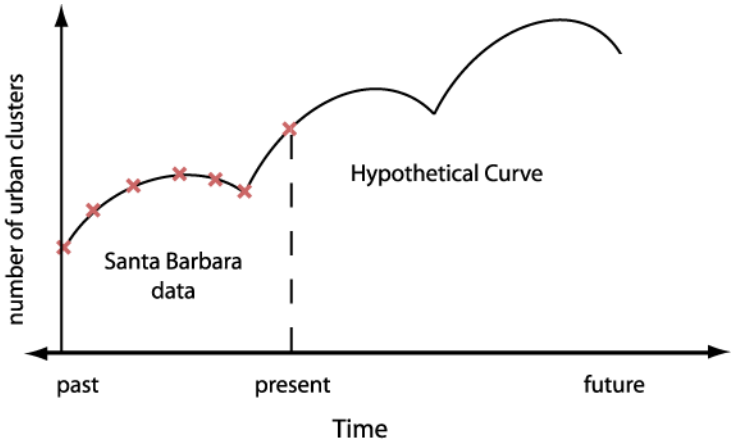

Figure 8-5: Hypothesis of size of urban clusters boom and bust cycles.

of boom and bust states of urban systems which is treated in SLEUTH through self-modification (Figure 8-5). Such hypotheses can be generated through the examination of historical data, tested with CA models, and can improve the theoretical basis of CA application. In turn, results will inform the fields of dynamic urban and CA modeling, provide a foundation for continued research and lead to the development of improved measurements to describe urban dynamics.

BIBLIOGRAPHY

Allen, P. M. (1997). "Cities and regions as evolutionary, complex systems." Geographical Systems 4(103-130).

Alonso, W. (1964). Location and Land Use, Harvard University Press.

Batty, M. (1976). Urban modeling: algorithms, calibrations, predictions. Cambridge, Cambridge University Press.

Batty, M. (1981). Urban Models. Quantitative Geography: a British view. N. Wrigley and R. J. Bennett. London, Routledge and Kegan Paul: 181-91.

Batty, M. (1991). Cities as Fractals: Simulating Growth and Form. Fractals and Chaos. A. J. Crilly, R. A. Earnshaw and H. Jones, Springer Verlag: 43-69.

Batty, M., H. Couclelis, et al. (1997). "Editorial: urban systems as cellular automata." Environment and Planning B 24: 159-164.

Batty, M. and P. A. Longley (1986). "The fractal simulation of urban structure." Environment and Planning A 18: 1143-1179.

Batty, M. and P. A. Longley (1987). "Fractal-based description of urban from." Environment and Planning B: Planning and Design 14: 123-34.

Batty, M. and P. A. Longley (1988). "The morphology of urban land use." Environment and Planning B 15: 461-488.

Batty, M., P. A. Longley, et al. (1989). "Urban growth and form: Scaling, fractal geometry, and diffusion-limited aggregation." Environment and Planning A 21: 1447-1472.

Batty, M. and Y. Xie (1999). "Modeling urban dynamics through GIS-based cellular automata." Computers, Environment and Urban Systems 23: 205-233.

Benati, S. (1997). "A cellular automaton for the simulation of competitive location." Environment and Planning B 24: 205-218.

Burroughs, P. A. (1981). "Fractal dimensions of landscapes and other environmental data." Nature 294: 240-242.

Candau, J. and K. C. Clarke (2000). Probabilistic Land Cover Transition Modeling Using Deltatrons. 2000 URISA Annual Conference, Orlando, FL.

Candau, J., S. Rasmussen, et al. (2000). A coupled cellular automaton model for land use/land cover dynamics. 4th International Conference on Integrating GIS and Environmental Modeling(GIS/EM4):Problems, Prospects and Research Needs, Banff, Alberta, Canada.

Carroll (1982). "National City-Size Distribution: What Do We Know After 67 Years of Research?" Progress in Human Geography IV: 1-43.

Casti, J. (1997). Would-be Worlds: How Simulation is Changing the Frontiers of Science. New York, John Wiley and Sons.

Cecchini, A. (1996). "Urban modelling by means of cellular automata: generalized automata with the help on-line (AUGH) model." Environment and Planning B 23(6): 721-732.

Clarke, K. C. and L. Gaydos (1998). "Loose-coupling a cellular automaton model and GIS: long-term urban growth prediction of San Francisco and Washington/Baltimore." International journal of geographical information systems 12(7): 699-714.

Clarke, K. C. and S. Hoppen (1997). "A self-modifying cellular automaton model of historical urbanization in the San Francisco Bay Area." Environment and Planning A 24: 247-261.

Clarke, K. C., S. Hoppen, et al. (1997). "Methods and techniques for rigorous calibration of a cellular automaton model of urban growth.".

Couclelis, H. (1985). "Cellular worlds: a framework for modeling micro-macro dynamics." Environment and Planning A 17: 585-596.

Couclelis, H. (1997). "From cellular automata to urban models: new principles for model development and implementation." Environment and Planning B 24(2): 165-174.

Dyckman, J. W. (1963). "The scientific world of the city planners." American Behavioral Scientist 6: 46-50.

Gabiax, X. (1999). "Zipf's Law ant the Growth of Cities." The American Econimic Review 89(2): 129-132.

Gabiax, X. (1999). "Zipf's Law for Cities: an explanation." The Quarterly Journal of Economics: 739-767.

Giudici, M. (2001). Development, calibration and validation of physical models. Geographic information systems and environmental modeling. K. C. Clarke, B. O. Parks and M. P. Crane. Upper Saddle River, NJ, Prentiss Hall: 100-121.

Goldstein, N. (2000). Do cities learn from getting burned? Artificial Life VII, Portland, OR.

Harvey, J. (1996). Urban Land Economics, Houndsmills.

Hester, D. (1999). Urban Dynamics of the Middle Rio Grande Basin. Denver, CO, US Geological Survey.

Horgan, J. (1995). "From Complexity to perplexity: Can science achieve a unified theory of complesity systems? Even at the Santa Fe Institute some researchers have their doubts." Scientific American.

Kivell, P. (1993). Land and the City: Patterns and processes of urban change. London, Routledge.

Kramer, J. (1996). Integration of a GIS with a local scale self-modifying cellular automaton urban growth model in Southeastern Orange County, NY. Department of Geography. New York, Hunter College: 73.

Krugman, P. (1996). "Confronting the Urban Mystery." Journal of the Japanese and International Economies, X: 399-418.

Krugman, P. (1996). The Self-Organizing Economy. Malden, MA, Blackwell.

Li, S. and A. Yeh (2000). "Modeling sustainable urban development by the integration of constrained cellular automata and GIS." International journal of geographical information systems 14(2): 131-152.

Longley, P. A., M. Batty, et al. (1990). "Shape Size and Dimension of Urban Settlements." Transactions, Institute of British Geographers 16(1): 75-94.

Liu (2001). Geographic information systems, cellular automata and fuzzy logic: 236.
Mayhew, S. (1997). Alonso mode. lA Dictionary of Geography, xrefer.com Oxford University Press. 2001.

Mayhew, S. (1997). Multiple nuclei model. lA Dictionary of Geography, xrefer.com Oxford University Press. 2001.

Nagel, K., S. Rasmussen, et al. (1996). Network traffic as self-organized critical phenomena, Los Alamos National Labs.

O'Sullivan, D. and P. Torrens (2000). Cellular Models of Urban Systems. Theoretical and Practical Issues on Cellular Automata, Proceedings of the Fourth International Connference on Cellular Automata for Research and Industry (ACRI 2000), Karlsruhe, Germany, Springer-Verlag, London.

Papini, L. and G. A. Rabino (1997). Urban Cellular Automata: an evolutionary prototype. ACRI '96: Proceedings of the Second Conference on Cellular Automata for Research and Industry, Springer Berlin.

Portugali, J. (2000). Self-Organization and the City. Berlin.

Portugali, J. and I. Benenson (1995). "Artificial planning experience by means of a heuristic cell-space model:simulating international migraton and the urban process." Environment and Planning A 27: 1647-1665.

Rosen, K. and M. Resnick (1980). "The Size Distribution of Cities: An Examination of the Pareto Law and Primacy." Journal of Urban Economics, VIII: 165-186.

Rozman, G. (1990). "East Asian Urbanization in the Nineteenth Century.".

Sanders, L., P. D, et al. (1997). "SIMPOP: a multiagent for the study of urbanism." Environment and Planning B 24: 278-305.

SBCAG (2001). Santa Barbara County 2030 Land and Population: The Potential Effects of Population Growth on Urban and Rural Lands. Santa Barbara, CA, Santa Barbara County.

Sembolini, F. (1997). "An urban and regional model based on cellular automata." Environment and Planning B 24: 589-612.

Sembolini, F. (2000). The dynamic of an urban cellular automata model in a 3-D spatial pattern. XXI National Conference Aisre: Regional and Urban Growth in a Global Market, Palermo.

Silva, E. A. and K. C. Clarke (forthcoming). "Calibration of the SLEUTH Urban Growth Model for Lisbon and Porto, Portugal." Environment and Planning B.

Stephenson, N. (1999). Cryptonomicon. New York, Avon Books.

Tobler, W. (1970). "A computer movie simulating population growth in the Detroit region." Economic Geography 42: 234-240.

Tobler, W. (1979). Cellular Geography. Philosophy in Geography. S. Gale and G. Olsson. Dordrect, The Netherlands, D. Reidel: 279-386.

Torrens, P. M. (2000). How Cellular Models of Urban Systems Work (1. Theory), Centre for Advanced Spatial Analysis
University College London
1-19 Torrington Place
Gower Street
London WC1E 6BT: 68.

Torrens, P. M. (2000). How Land-Use-Transportation Models Work. London, Centre for Advanced Spatial Analysis.

Ward, D., A. Murray, et al. (2000). "A stochastically constrained cellular model of urban growth." Computers, Environment and Urban Systems 24: 539-558.

Webster, C. J. and F. Wu (1999). "Regulation, land use mix and urban performance part 1. Performance." Environment and Planning A 31(8): 1433-1442.

Webster, C. J. and F. Wu (1999). "Regulation, land use mix and urban performance part 2. Theory." Environment and Planning A 31(9): 1529-1547.

White, R. and G. Engelen (1993). "Cellular automata and fractal urban form." Environment and Planning A 25: 1175-1199.

White, R. and G. Engelen (1997). "Cellular automata as the basis of integrated dynamic regional modeling." Environment and Planning B 24: 323-343.

White, R. and G. Engelen (2000). "High-resolution integrated modeling of the spatial dynamics of urban and regional systems." Computers, Environment and Urban Systems 24(383-400).

White, R., G. Engelen, et al. (1997). "The use of constrained cellular automata fro high-resolution modelling of urban land use dynamics." Environment and Planning B 24: 323-343.

White, R., G. Engelen, et al. (1993). Cellular automata modelling of fractal urban land use patterns: forecasting change for planning applications. 8° European Colloquium on Theoretical and Quantitative Geography, Budapest.

Wu, F. (1998). "An experiment on the generic polycentricity of urban growth in a cellular automatic city." Environment and Planning B 25(731-752).

Wu, F. (1999). A simulation approach to urban changes: experiments and observations on fluctuations in cellular automata. Sixth International Conference on Computers in Urban Planninge and Urban Management, Venice, Italy.

Zipf, G. (1949). Human Behavior and the Principle of Least Effort. Cambridge, MA, Addison-Wesley.

GLOSSARY

Avg.log. a SLEUTH output file. It contains measured values of simulated data averaged over Monte Carlo iterations for every run and control year.
Base statistics. The measurements taken from the control year data.
Best solution set. (BSS) The goal of model calibration. The average of each of the five coefficient values from the final simulated year of the derive run. These are used to initialize a forecast run.
BOOM. Self-modification parameter applied to the dispersion, breed and spread coefficients when the system is in a boom state.
Boom state. A state of accelerating urban growth entered into the when the urban growth rate exceeds the *CRITICAL_HIGH*.
BSS. See (Best solution set).
BUST. Self-modification parameter applied to the dispersion, breed and spread coefficients when the system is in a bust state.
Bust state. A state of decelerated urban growth entered into the when the urban growth rate goes below the *CRITICAL_LOW*.
Coarse phase. See Calibration phase.
Calibration Mode. An automated process of searching through the model coefficient space to find a set which best describes historical urban change for a study area. Coefficient sets are generated using the coefficient start, step and stop values defined in the scenario file. Each set initializes a run.
Calibration phase. One of three steps in brute force calibration (coarse, fine, and final) through which coefficient ranges are narrowed. See section 3.2 for more information.
Coefficient start value. Initial coefficient value for a model run. The low value of a coefficient range.
Coefficient step value. In calibration, an increment value which is added to the start value iteratively for all possible permutations of given ranges and increments.
Coefficient stop value. Final coefficient value for a model run. The high value of a coefficient range.
Control year. A date for which urban data exists in the historical database. An urban layer from the historical database.
CRITICAL_HIGH. The threshold for the urban growth rate above which a boom state exists for the system and self-modification will be applied to the coefficients.
CRITICAL_LOW. The threshold for the urban growth rate below which a bust state exists for the system and self-modification will be applied to the coefficients.
Derive run. Initialized with the set of best coefficients selected from the calibration phases, a large number of Monte Carlo simulations are used to simulate growth for the time period represented in the historical database. From this run, averaged values of the calibration metrics and coefficient values for the control years may be derived

for analysis. Most importantly, the averaged coefficient values from the final control year (BSS) are used to initialize a calibrated forecast run.

Final phase. See Calibration Phase.

Fine phase. See Calibration Phase.

Forecast mode. Initialized with the most recent image data, will perform a single run, in Monte Carlo fashion, using the calibrated BSS for initialization.

Growth Cycle. The basic unit of SLEUTH execution. It begins by setting each of the coefficients to a unique value. Each of the growth rules are then applied. Finally, the resulting growth rate is evaluated. If the growth rate exceeds or falls short of the *CRITICAL_HIGH* or *CRITICAL_LOW* values, model self-modification is applied. Self-modification will slightly alter the coefficient values to simulate accelerated or depressed growth that is related with boom and bust conditions in urban development.

Prediction Mode. See forecast mode.

ROAD_GRAV_SENSITIVITY. A change value that is applied to the road gravity coefficient during self-modification.

Run. An execution of SLEUTH that begins with a single set of coefficient values, and performs a designated number of Monte Carlo iterations. May be followed by another run (as in calibration) or finish at the end of the Monte Carlos (as in forecasting).

Scenario file. The SLEUTH execution file.

Self-modification. A process of slightly altering SLEUTH coefficient values to simulate accelerated or depressed growth that is related with system-wide boom and bust conditions in urban development.

SLOPE_SENSITIVITY. A constant value that is applied to the slope resistance coefficient during self-modification.

Start date. The first year represented by SLEUTH simulation. In Calibration this date corresponds with the date of the earliest (most historical) urban layer. In Forecasting it will correspond to the START_DATE value defined in the run's scenario file, which must also be the date of the most recent urban layer.

Stop date. The final year represented by SLEUTH simulation. In Calibration this date corresponds with the date of the most recent urban layer. In Forecasting it will correspond to the STOP_DATE value defined in the run's scenario file.

Simulation. A simulation is a series of growth cycles that begins at a start date and completes at a stop date.

APPENDIX A

Examples of input data for the South Coast GIS database

urban 1929

urban 1943

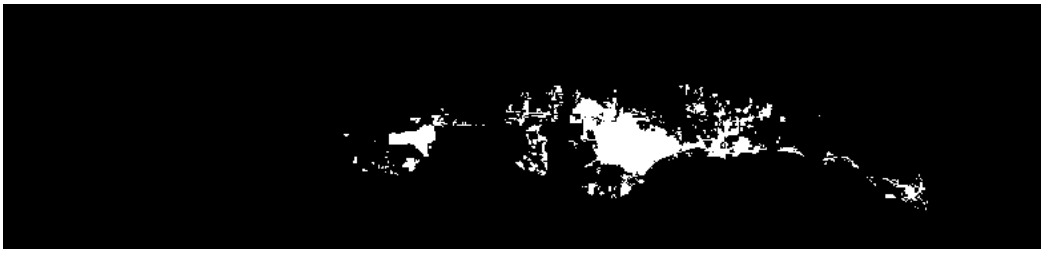

urban 1954

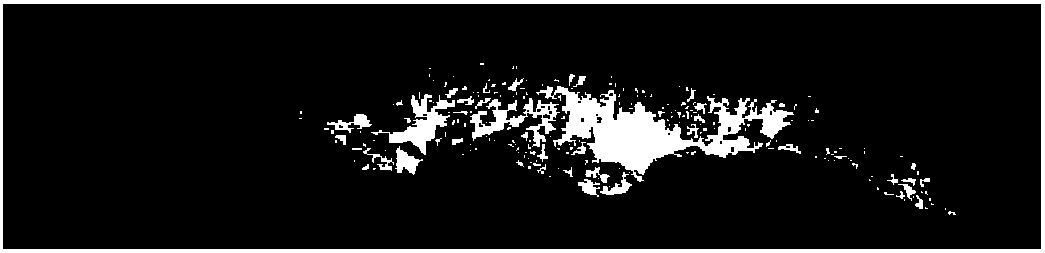

urban 1967

urban 1976

urban 1986

urban 1998

roads 1929

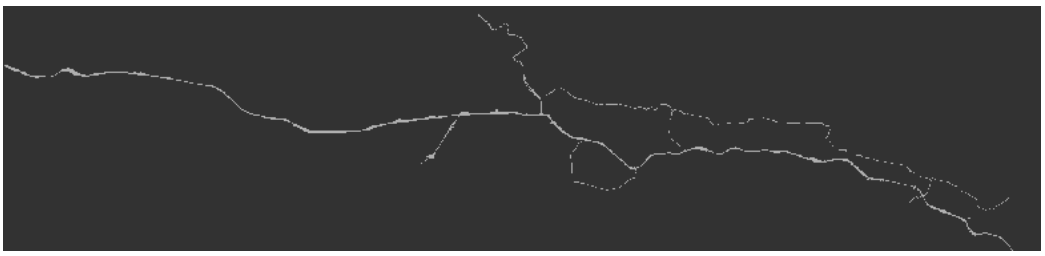

roads 1943

roads 1957

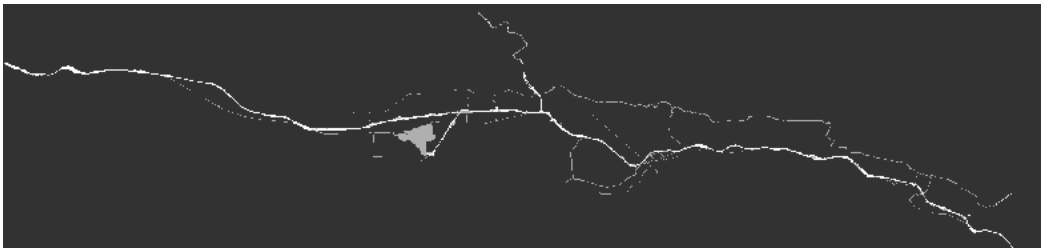

roads 1967

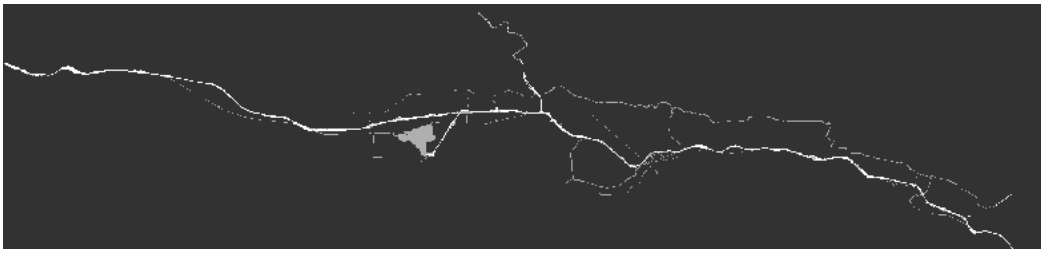

roads 1976

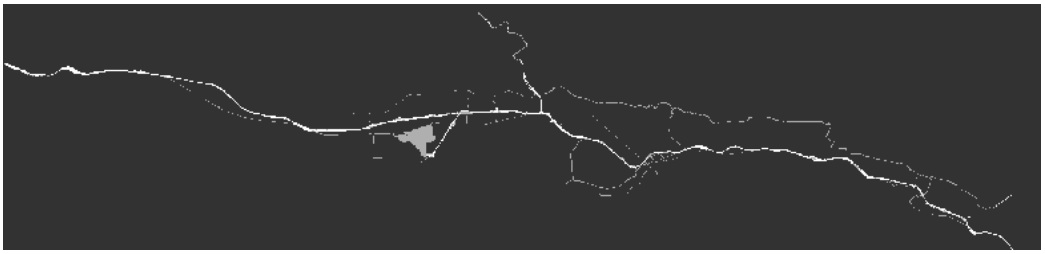

roads 1986

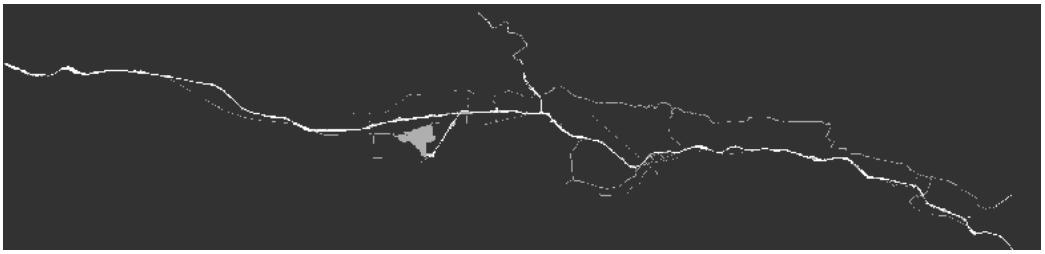

roads 1998

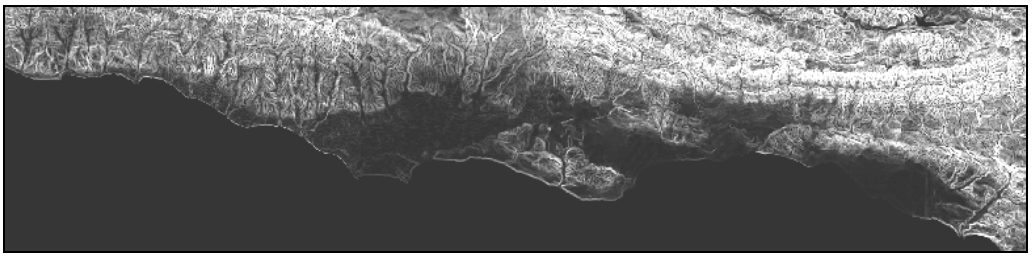

slope

exclusion

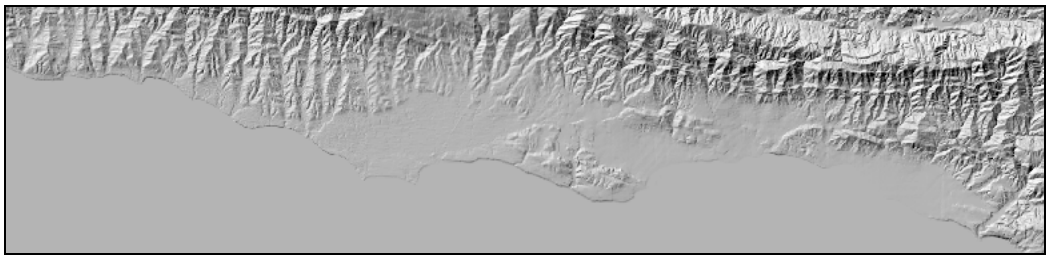

hillshade

APPENDIX B

SLEUTH initialization values from all phases of the three calibration scenarios:

Self-modification constants and coefficient range/interval selection tables

Self-modification Constants

CRITICAL_LOW	0.97
CRITICAL_HIGH	1.3
BOOM	1.01
BUST	0.9
SLOPE_SENSITIVITY	0.1
ROAD_GRAV_SENSITIVITY	0.01

Cal1, Cal2 Cal3 Coarse set-up

	Range			
Coeff	start	stop	step	**Count**
disp	0	100	25	5
breed	0	100	25	5
spread	0	100	25	5
slope	0	100	25	5
road grav	0	100	25	5

Cal1 Fine Set-up

		Range			
Coeff	**Best**	start	stop	step	**Count**
disp	1	0	12	4	4
breed	75	75	99	6	5
spread	25	25	75	10	6
slope	100	25	100	15	6
road grav	75	51	75	6	5

Cal1 Final Set-up

		Range			
Coeff	**Best**	start	stop	step	**Count**
disp	1	1	5	1	5
breed	87	87	99	3	5
spread	75	66	75	3	5
slope	65	35	75	8	6
road grav	57	57	69	3	5

Cal1 Derive Set-up/Results

Coeff	**initial**	**completed**
disp	1	2
breed	90	100
spread	69	100
slope	51	1
road grav	57	70

Cal1 Forecast

Coeff	**initial**	**completed**
disp	2	1
breed	100	15
spread	100	15
slope	1	100
road grav	70	65

Cal2 Fine Set-up

		Range			
Coeff	**Best**	start	stop	step	**Count**
disp	50	26	50	6	5
breed	25	25	49	6	5
spread	100	76	100	6	5
slope	100	76	100	6	5
road grav	50	0	50	10	6

Cal2 Final Set-up

		Range			
Coeff	**Best**	start	stop	step	**Count**
disp	26	26	35	2	5
breed	31	25	33	2	5
spread	88	88	96	2	5
slope	82	76	84	2	5
road grav	20	10	20	2	6

Cal2 Derive Set-up/Results

Coeff	**initial**	**completed**
disp	30	40
breed	31	41
spread	96	100
slope	76	1
road grav	14	23

Cal2 Forecast

Coeff	**initial**	**completed**
disp	40	38
breed	41	39
spread	100	85
slope	1	93
road grav	23	19

Cal3 Fine Set-up

		Range			
Coeff	**Best**	start	stop	step	**Count**
disp	1	0	12	4	4
breed	75	75	75	15	6
spread	100	100	100	6	5
slope	1	25	25	6	5
road grav	25	25	75	6	5

Cal3 Final Set-up

		Range			
Coeff	**Best**	start	stop	step	**Count**
disp	8	8	12	1	5
breed	75	45	75	6	5
spread	100	76	88	3	5
slope	25	9	25	4	6
road grav	19	0	25	5	6

Cal3 Derive Set-up/Results

Coeff	initial	completed
disp	11	7
breed	63	38
spread	88	38
slope	25	49
road grav	25	34

Cal3 Forecast

Coeff	initial	completed
disp	7	1
breed	38	1
spread	38	1
slope	49	100
road grav	34	20

APPENDIX C

SLEUTH calibration regression scores from the derive runs of All_data, Recent_data, and Sparse_data.

Cal1 Regression Scores

	Coarse	Fine	Final
pop	0.98	0.98	0.98
edges	0.84	0.78	0.78
cluster	0.92	0.92	0.92
cluster size	0.93	0.86	0.86
Lee Salee	0.39	0.47	0.47
Product	0.28	0.29	0.29

Cal2 Regression Scores

	Coarse	Fine	Final
pop	0.92	0.94	0.95
edges	0.96	0.98	1.00
cluster	0.87	0.96	0.97
cluster size	1.00	0.93	0.99
Lee Salee	0.70	0.71	0.71
Product	0.54	0.59	0.64

Cal3 Regression Scores

	Coarse	Fine	Final
pop	0.99	0.98	0.97
edges	0.83	0.95	0.98
cluster	0.99	1.00	1.00
cluster size	0.94	0.91	0.91
Lee Salee	0.46	0.47	0.47
Product	0.35	0.40	0.40

GLOSSARY